AD-A050 877 BRITISH COLUMBIA UNIV VANCOUVER INST OF OCEANOGRAPHY F/G 14/2
THE DESIGN AND PERFORMANCE OF FREE-FALL MICROSTRUCTURE INSTRUME--ETC(U)
OCT 77 T R OSBORN N00014-76-C-0446
UNCLASSIFIED IOUBC-MS-30 NL

| OF |
AD
A050 877

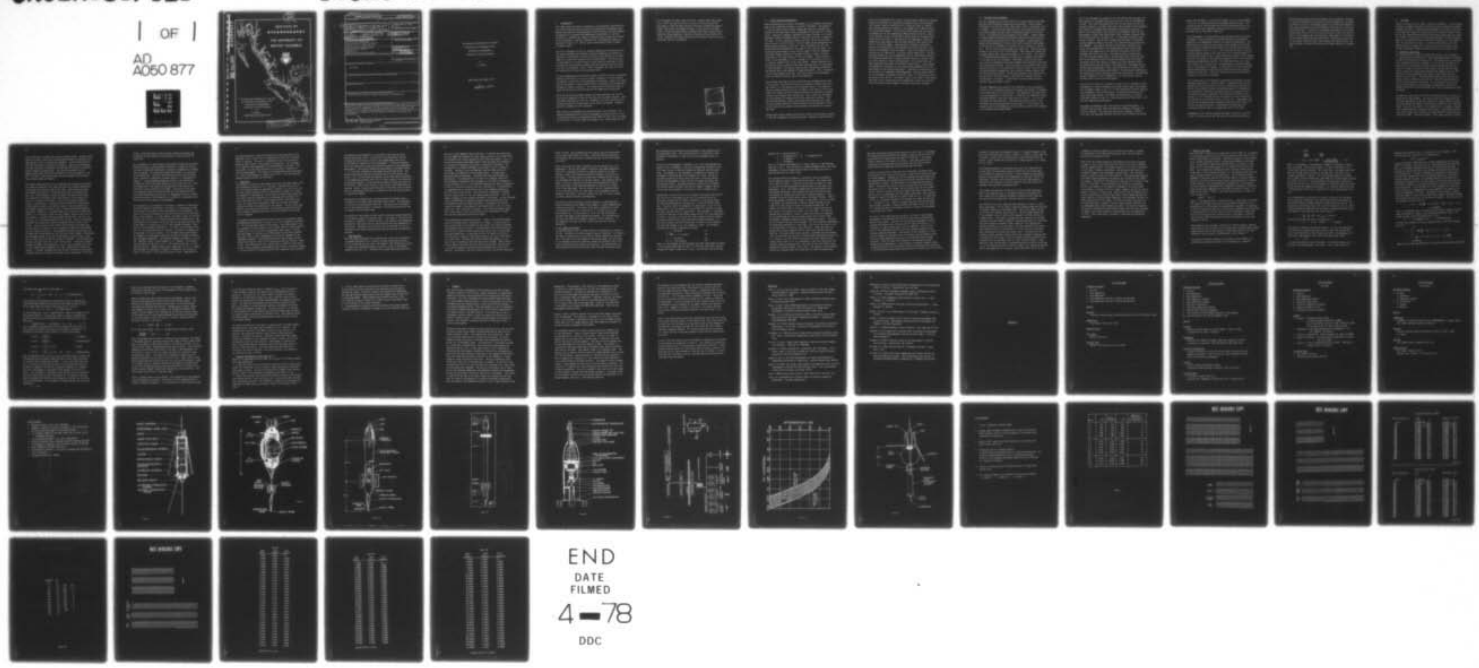

END
DATE
FILMED
4-78
DDC

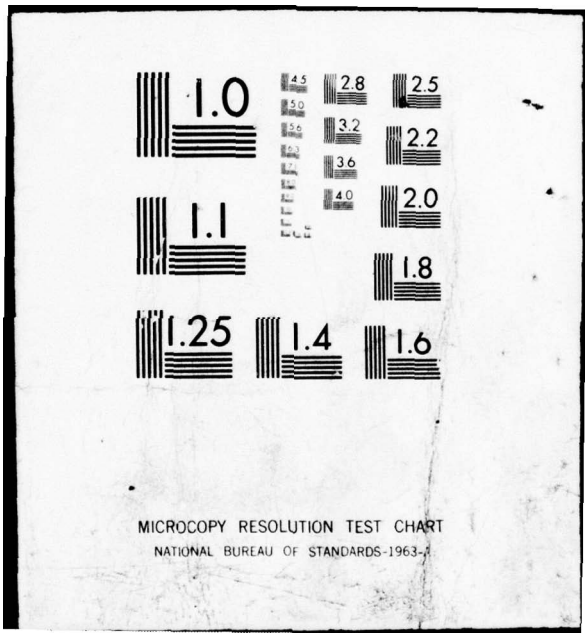
1.0
1.1
1.25
1.4
1.6
1.8
2.0
2.2
2.5
2.8
3.2
3.6
4.0
4.5
5.0
5.6
MICROCOPY RESOLUTION TEST CHART
NATIONAL BUREAU OF STANDARDS-1963-A

AD A050877
DDC FILE COPY

12

INSTITUTE OF OCEANOGRAPHY

THE UNIVERSITY OF BRITISH COLUMBIA

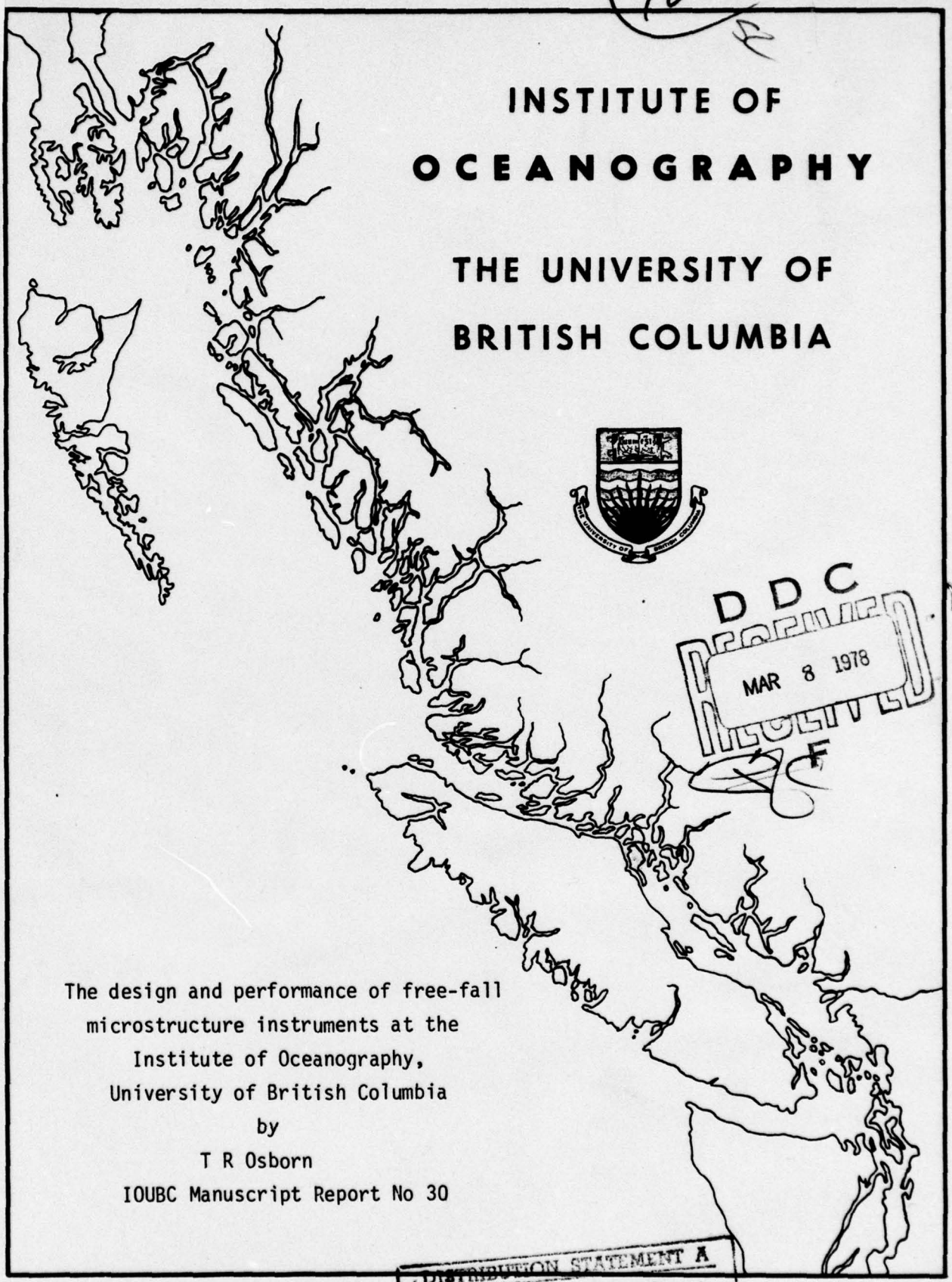

DDC
RECEIVED
MAR 8 1978
F

The design and performance of free-fall microstructure instruments at the Institute of Oceanography, University of British Columbia

by

T R Osborn

IOUBC Manuscript Report No 30

DISTRIBUTION STATEMENT A
Approved for public release;
Distribution Unlimited

UNCLASSIFIED

SECURITY CLASSIFICATION OF THIS PAGE (When Data Entered)

REPORT DOCUMENTATION PAGE

READ INSTRUCTIONS BEFORE COMPLETING FORM

1. REPORT NUMBER

2. GOVT ACCESSION NO.

3. RECIPIENT'S CATALOG NUMBER

4. TITLE (and Subtitle)

(6) THE DESIGN AND PERFORMANCE OF FREE-FALL MICRO-STRUCTURE INSTRUMENTS AT THE INSTITUTE OF OCEANOGRAPHY, UNIVERSITY OF BRITISH COLUMBIA,

5. TYPE OF REPORT & PERIOD COVERED
IOUBC Manuscript Report No. 30 ✓

6. PERFORMING ORG. REPORT NUMBER

7. AUTHOR(s)

T.R. Osborn (14) IOUBC MS-30

(10) Thomas R. Osborn

8. CONTRACT OR GRANT NUMBER(s)

(15) N00014-76-C-0446 ✓
NR 083-207

9. PERFORMING ORGANIZATION NAME AND ADDRESS

Institute of Oceanography
The University of British Columbia ✓
Vancouver, B.C., Canada V6T 1W5

10. PROGRAM ELEMENT, PROJECT, TASK AREA & WORK UNIT NUMBERS

11. CONTROLLING OFFICE NAME AND ADDRESS

Office of Naval Research
ONR Code 481
NSTL Station, Mississippi 39529

12. REPORT DATE

(11) Oct 77

13. NUMBER OF PAGES

55 (12) 59p.

14. MONITORING AGENCY NAME & ADDRESS (if different from Controlling Office)

15. SECURITY CLASS. (of this report)

15a. DECLASSIFICATION/DOWNGRADING SCHEDULE

16. DISTRIBUTION STATEMENT (of this Report)

Unlimited

17. DISTRIBUTION STATEMENT (of the abstract entered in Block 20, if different from Report)

18. SUPPLEMENTARY NOTES

19. KEY WORDS (Continue on reverse side if necessary and identify by block number)

Microstructure, Free-fall design, Performance, Instrumentation.

20. ABSTRACT (Continue on reverse side if necessary and identify by block number)

This report covers the design, manufacture, and operational characteristics of the four different types of free-fall microstructure instruments developed at the Institute of Oceanography of The University of British Columbia. The objective is to produce one comprehensive description of the four vehicles as a reference for readers of material based on the data collected by the instruments.

DD FORM 1 JAN 73 1473 EDITION OF 1 NOV 65 IS OBSOLETE
S/N 0102-LF-014-6601

SECURITY CLASSIFICATION OF THIS PAGE (When Data Entered)

063 770 JUB

The design and performance of free-fall microstructure instruments at the Institute of Oceanography, University of British Columbia

by

T.R. Osborn

IOUBC Manuscript Report # 30

October 1977

I Introduction

This report covers the design, manufacture, and operational characteristics of the four different types of free-fall microstructure instruments developed at the Institute of Oceanography of the University of British Columbia. The objective is to produce one comprehensive description of the four vehicles as a reference for readers of material based on the data collected by the instruments. Detailed information for the temperature sensors is available in Lueck et al. (1977), and for the velocity probes in Osborn & Crawford (1977).

The first instrument was used for studying temperature microstructure only. The second instrument was designed to measure temperature and electrical conductivity fluctuations, as well as being the test vehicle for the development of a sensor for turbulent velocity measurements. With the successful development of a velocity probe, a branch point in the study of microstructure was reached where everything that was planned could not be done with just one instrument. Thus, a third instrument, the Camel, was built to further only the velocity microstructure work.

The early temperature microstructure studies, with the first two instruments, showed the desirability of a set of simple instruments to look at spatial and temporal variability of the temperature fluctuations. Hence, the fourth design, the Pumpkin, of which three identical instruments were constructed, was made as simple as possible. This design allows for multiple drops to study the variation in time and space of the temperature fluctuations.

While four distinct instrument formats have been developed, the last two are the most important in terms of the data that have been collected. Thus, the report describes the first two instruments, but their characteristics are not discussed in as much detail as the latter two designs. Appendix I contains a synopsis of each instrument.

Other free-fall instruments have been described in the literature. For ocean microstructure work the early development was mainly due to C.S. Cox at Scripps Institution of Oceanography (see Osborn and Cox, 1972, and Gregg and Cox, 1971). Williams (1974) and Caldwell et al. (1975) describe free-

fall instruments for small-scale profiling. Simpson (1972) and Sanford et al. (1977) use free-fall bodies to look at the velocity profiles with depth, a field now being studied by Williams at Woods Hole Oceanographic Institution, and Rossby and Evans at the University of Rhode Island. Elliot and Oakey (1976), and Oakey (1977) have a sophisticated system for doing temperature, electrical conductivity and velocity profiling. Mortensen and Lange (1976) discuss the design criterion for wing stabilized free-fall instruments.

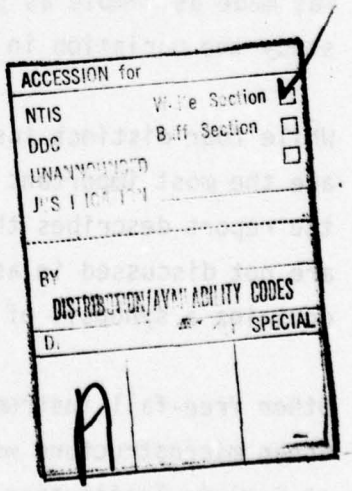

II Initial Design Considerations

Before discussing the individual instruments, it is worthwhile considering some of the constraints placed on a free-fall instrument. The objective is to have a vehicle which travels through the ocean at a constant rate relative to the local water column, independent of the motion of a surface vessel. Because of frequency limitations on sensor response, it is often desirable to have the descent speed less than the 1 m/s that is common for STD casts. In fact, speeds are usually less than .50 m/s and for some workers as low as .03 or .04 m/s. The fall speed can be regulated by the excess weight, the drag, or the lift. Cox's instruments use the lift derived from the autorotation of the wings to limit the fall speed. Reducing the excess weight to get a low fall speed is difficult because a fractional change in density of the water produces a change in excess weight that is the same fraction of the *total* weight. Thus, having balanced a 70 kg instrument to .5 kg, a change of .1% in density (1 unit in σ_t) causes a change of 14% in the excess weight. Another technique is to increase the drag by increasing the cross-sectional area (i.e. form drag) of the instrument. Care must be taken to avoid introducing unfavorable body motions due to the shedding of large-scale eddies. Thus, a parachute or flat plate should not be used. Even blunt ends on vertical measure cases can cause oscillations due to flow separation.

Upon reaching some lower limit for profiling, the instrument must return to the surface. Hence the vehicle must be buoyant at depth as well as at the surface (i.e. the buoyancy must be pressure-proof). The problem of making a buoyant pressure case for all depths in the ocean is non-trivial. Brown & Cox (1973) give the information necessary to determine a suitable pressure case designed from aluminum pipe. Our original two instruments use glass spheres for buoyancy and for the electronics housings. While the available buoyancy, volume, and maximum depth characteristics make the glass spheres attractive, these observers find the problems of access to the inside of the pressure housing exceed the advantages for development work.

Another major design problem with free-fall oceanic microstructure systems is the data recording or transmitting system. Because of the small-scale

nature of the phenomenon under study, detailed spatial sampling is required. Velocity fluctuations can reasonably be expected down to the centimetre scale, hence a spatial resolution of 10^2 cycles per metre is required. That resolution requires or implies 2×10^5 numbers for a 1000 m profile for each channel sampled. If one has two data channels for the velocity and another two for the temperature gradient and the electrical conductivity gradient, as well as additional storage space for the mean values (which can be digitized at lower densities) of temperature, electrical conductivity, and pressure, then the total amount of data could be 10^7 bits at 10 bits per number. That estimate is probably conservative because of the desirability of having more than 10 bits per word. Now the data rate depends on the fall speed. Given a fall speed of 10 cm/s the data rate is 1000 bits/s. Fifty cm/s implies 5000 bits/s. The data handling problems are not insurmountable but are significantly difficult. Cox solved the problem with a hybrid recording that put a digital signal on a multi-channel ¼" tape in analog fashion. This system limits the depth range over which data are recorded to about 150 m. It was decided to telemeter the information to the surface using expendable wire links manufactured by the Sippican Corporation. These XWLs are essentially the wire portion of an expendable bathythermograph. With one spool located on the instrument and another on the ship, there is little drag to affect the motion of the vehicle. The dynamic range of our system is much smaller than that in Cox's system and we have compensated in part for this deficiency with more analog treatment of the data inside the instrument.

III The First Two Instruments

The first instrument built at UBC (see Fig. 1) was designed in late 1969 and early 1970 to measure temperature microstructure. The instrument consisted of a cylindrical plastic outer shell 1.05 m in length and .28 m in diameter. Inside the outer housing was a .25 m diameter Corning polar access glass sphere that was used as the pressure housing for the electronics. The electronics were attached to the 'endcap'. Another sphere and some syntactic foam were also mounted inside the cylindrical housing to provide sufficient flotation for the instrument. An Ocean Applied Research (OAR) submersible citizen's band radio transmitter was mounted on the top of the instrument for locating it after returning to the surface. The wire link was also mounted on the upper end. Three wings were mounted to the outer rim of the instrument. These wings were formed from salvaged sonobuoy wings that were extended to .97 m length. The release is a Richardson-type stretched pin release and is mounted at the center of the lower end of the instrument. The weight is held on with wires that run out to compressed salt blocks mounted on the outside of the lower end of the plastic housing. Thus, the weight can be dropped either by the breaking of the pin or the dissolving of the salt blocks. The salt blocks are much preferable to magnesium links as back-up releases because they are quicker and more certain. Unlike some magnesium links, they are not coated by their corrosion products, hence are not protected from the desired decay in sea water. If more than 45 minutes before release is required, they are dipped in paint.

The water temperature was sensed by two thermistors; one was mounted on the axis of the instrument housing and the other was mounted ½ m outboard, at the same level as the central probe. The temperature from each thermistor was telemetered to the surface. In addition, the temperature signal was passed through a high pass single pole R-C filter (τ = ½ s) in the instrument and then amplified. These amplified signals (one for each thermistor) were then transmitted to the surface. A fifth signal, the pressure, was also telemetered up to the surface so that the fall speed of the instrument could be determined.

This first instrument was essentially the test bed for two new ideas, the glass spheres as instrument housings and the wire links for telemetering the data. The latter idea worked quite well but the former was not very successful because of the small entry hole into the sphere (63 mm diameter). Data from this instrument were analyzed for two projects, the work in Rupert Inlet (during March 1971) described by Drinkwater (1973) and the measurements in Powell Lake (during Sept. 1971) reported by Osborn (1973). The instrument was lost in Powell Lake. It resurfaced 11 months later, and was recovered from the local resident who had found it and called the phone number printed on the side of the outer housing just below the word 'REWARD'. The pressure release pin had broken, indicating that either the instrument had hit the bottom shortly after the pin broke, or the pin had snapped due to the continual high pressure while the instrument was stuck in the mud. The previous drop to the one which lost the instrument showed signs of scraping the bottom (there was sediment in the thermistor holder although the thermistor was not broken). The bottom of the lake contains no oxygen but rather hydrogen sulfide. The orange outer paint had turned a dark green color, the copper wire on the XWL spool had darkened in color, and the potting at the base of the OAR radio transmitter antenna had softened. The potting was replaced and the transmitter has been used many times since the recovery. The Vibrotron pressure transducer in the instrument was still good and was used by Galloway (1974) in one of his tide gauges.

With the loss of the first instrument in Powell Lake in September of 1971, development of a second instrument, which had already begun, was hastened. This instrument, shown in Fig. 2, is in the configuration finally used for the development of the velocity probe. The pressure housing was a 16" polar access glass sphere. The sphere was chosen because it offered sufficient flotation as well as a high maximum pressure rating and a .12 m hole for inserting the electronics.

The sphere was mounted inside a PVC frame with the endcap upward. A flashing light and radio (both from OAR) were mounted on the upper end to aid in recovery. The wings were again from a sonobuoy, initially .28 m long, but shortened from their original size to reduce the rotation

rate of the instrument. At their final length of .12 m, they produced little lift, so the balancing of the instrument became critical. The original design of the instrument was with the larger wings and an outboard thermistor again mounted ½ m from the axis of the instrument at the same level as the central thermistor.

A few improvements in the electronics were introduced with this second instrument. The most notable was the modification of the high-pass amplifier of the temperature signal to a straight differentiator. This modification was really just an increase in the frequency of the high-pass filtering to something greater than 40 Hz from the previous value of approximately 1/3 Hz (τ = ½ s). This transition was done in steps so that the changing nature of the signal due to the increasing amount of differentiation could be seen. Another channel was added in which compensation for the effect of the thermistor attenuation was tried by boosting the measured temperature gradient in the band above 15 Hz, by an additional factor of ω to make up for the approximately single-pole attenuation of the thermistor's response. A correction of this sort required a detailed understanding of the thermistor attenuation; hence, the work reported in Lueck et al. (1977) was undertaken to study the thermistor response as a function of frequency.

The rotation rate of the instrument was measured electronically using a technique suggested by T. Sanford of WHOI. A permeable metal core was wrapped with a coil made from an XBT wire and the signal amplified so that as the instrument rotated, the changing magnetic flux through the coil generated an essentially sinusoidal curve as a function of time. This device proved very successful for measuring the rotation rate. A similar coil was installed with the axis vertical to look for possible oscillations of the instrument about a vertical axis. Experiments with a series of salinometers were conducted by IOUBC during the winter of 1971-72, but were unsuccessful in developing a sensing head with sufficient resolution and a low enough noise level to be useful.

Development of this second instrument was begun in earnest in the fall of 1971. By the spring of 1972 the work with the velocity probe was

sufficiently promising that the salinometer work was shelved. The mount for the second thermistor was removed to reduce asymmetries of the body, and from this time on a considerable amount of our effort was devoted to shear probe development, and the manufacture and setting up of the associated electronics. The probe first operated successfully in July 1972. By the August 1972 sea trip, from which data Osborn (1974) describes the probe, it was apparent that the large glass sphere made it too difficult to service and trouble-shoot the electronics. Additionally, the desire for more static stability made a new instrument housing desirable. The next instrument, the Camel, was designed and began operating in December 1972.

IV The Camel

Figures 3a and 3b show the 'Camel', the third instrument. It was designed primarily to support the velocity probe and initially expected to operate no deeper than 300 m. Operations were expected to be limited to the local inlets where the effects of surface waves can be ignored in terms of ship motion, thus handling problems during launch and recovery would be minimal. As a result of the success of the velocity probe work, studies were undertaken in the Equatorial Atlantic from the R V Atlantis II in the summer of 1974, off the Azores from the W F S Planet in March 1975, and in the western Atlantic on board the R V Knorr, as part of the Fine and Microstructure Experiment (FAME) organized by Drs Sanford and Hogg of WHOI.

A Mechanical construction

The pressure housing is 6061-t6 schedule 40 aluminum, .168 m diameter, 7.1 mm thickness and length 2.85 m. Maximum operating depth is estimated as 1000 m from the work of Brown and Cox. The endcaps are cut from 50-mm-thick aluminum plate, have a diameter of .20 m, and are attached to the tube with bolts to external lugs that have been welded onto the tube. There is a single O-ring seal to the inside of the tube which has been ground circular by a local marine engine-boring company, since no local machine shop could accommodate the length on their lathe and still machine a circular hole. The endcaps were machined after the tube was ground so that a proper seal was assured. Electrical penetrations are made via Electro-Oceanics connectors. All the electronics are inside the main case except for the temperature, conductivity, and velocity sensors and the velocity probe pre-amplifier, which is mounted just above the probe.

The upper and lower ends are faired with fiberglass shells to reduce the wobble due to eddy shedding. The brushes form a drag element that does not shed large eddies, so the fall speed can be reduced without reducing the excess weight and without causing large variations of fall speed with depth. There are six brushes, .17 m long and .16 m in diameter, mounted as an almost continuous ring around the cylinder. The brushes are held away from the body with triangular PVC plates mounted to the housing with large hose clamps. The whole assembly is then wired together to prevent

loss in the case of a sharp blow from the recovery vessel. An OAR flashing light and citizen's band radio (reduced antenna model) are mounted on the upper endcap to aid in locating the instrument. A Helle PG-06 pinger is used when the bottom is shallower than 1000 m. There are two rope hoops that were installed for operations in 1974 from the Atlantis II along the Atlantic Equatorial Undercurrent. The recovery procedure involves snagging these ropes with a hook attached to a line on the end of a long pole. The pole is then pulled loose and the instrument hoisted aboard (see Williams (1974) for details).

The release system consists of two Richardson-type stretched pin releases. The weights are mounted in two tubes and wires are stretched between the two releases and across the ends of the tubes. When either pin breaks, both weights are released. For safety, salt blocks are inserted into each line. These dissolve in about 45 minutes and release the weights. The instrument is ballasted so that the release of *either* weight will allow it to return to the surface. (On our first recovery along the equator in the Atlantic, it returned with one weight still attached and a small amount of water in the pressure case.) The only problem with the release system occurred on a cruise in Howe Sound with the bottom at about 200 m. Normally, a tin-plated copper wire is used for holding the weights in. On this trip, steel wire was brought, which was too stiff to work properly, so copper wire was borrowed from the ship. This wire was very soft, so a much larger diameter had to be used. That in turn reduced the amount the release screw could be threaded into the piston on the release. Thus, on one drop the release screw stripped its threads without breaking off its head, and the instrument hit bottom and stuck before the salt releases could work. The telemetering system indicated that the instrument was on the bottom and that the case had not flooded. Fortunately, the instrument worked its way out of the bottom in about 24 hours, after the salt blocks had dissolved and released the weights. The instrument was picked up two days later with a small cabin cruiser. The acoustic pinger had been included on the instrument in case of such a problem, and we had in fact already made arrangements for a small submersible to effect the recovery. A further safeguard that has not been instituted in the present instrument would be to modify the releases to drop the weights if the screw

strips. This modification could be simply effected by changing the orientation of the release so that the wires are trying to pull the screws out.

The salinometer is a modification of the design of Gregg and Cox (1971). Rather than using a spring mechanism that pulls a piston up a tube to suck water through the sensing port, a bellows is expanded at a constant rate with depth. The system that expands the bellows is a piston and spring combination. The piston has water on one side, with the other side at essentially atmospheric pressure because it is connected to a reservoir. A spring mounted between the reservoir and the bellows balances the force of the water pressure on the piston (Fig. 4). Thus, the compression of the spring and the expansion of the bellows are essentially linear functions of the depth. Variations in fall speed are unimportant since the volume of water per unit depth pulled into the bellows through the sensing port, is independent of the fall speed. Further discussion of the system will be reserved for presentation with the results of the conductivity measurements.

For the analysis of the behavior of the body in response to large-scale shears and velocity fluctuations in the ocean, it is necessary to know the location of the center of mass and buoyancy of the instrument. The center of mass can be measured by finding the balance point of the instrument in the laboratory. For the complete instrument, except for the drop weights, the C of M is 41 cm below the middle of the aluminum tube. The drop weights for the recent cruises have been 9.6 kg total mass with their center about 1.1 m below the C of M for the unloaded instrument. Thus, the C of M for the whole instrument is .13 m lower for the loaded instrument, or .54 m below the center of the tube. The center of buoyancy can be estimated in a similar fashion. The instrument housing and endcaps are symmetric in displacement except for the section inserted to contain the salinometer mechanisms. This apparatus weighs 167 Newtons in air and 100 Newtons in water, so the buoyancy is .67 Newtons. The distance from the center of the tube is 1.7 m. The recovery aids, etc., on the upper end have 40 Newtons buoyancy and a moment arm of 1.6 m. A reasonable estimate for the center of buoyancy is therefore .08 m below the center of the tube, or .46 m above the center of mass. Measurements of

the torque necessary to make the instrument lie horizontal while fully submerged yield a value of 370 ± 8% Newton-metres about the calculated center of buoyancy. The error is predominantly due to the problem of measuring small forces in the presence of wave motion. The instrument is so large that the measurements must be performed in the ocean. Even small waves in an enclosed yacht basin lead to errors of about 6% in the force measurements. The torque of 370 Newton-metres would correspond to a force of 804 Newtons at a moment arm of .46 m. The calculated and measured stability values are consistent.

B Electronics

The electronics consists of the measuring circuits, the power supply, and the telemetering system (Fig. 5). The power is derived from a set of Gel-Cell batteries which are regulated to a nominal ± 15 volts and a set of nickel-cadmium batteries that are regulated to a nominal + 6.3 volts. The telemetry is performed by a set of Sonex TEX-3075 voltage controlled oscillators specially designed to be low voltage and low current (6.3 volts rather than 28 volts). The FM signals from the individual oscillators are summed with an operational amplifier and then transformer-coupled to the XWL for transmission to the surface. The only signal that does not use an auxiliary oscillator is the pressure signal which comes from a pressure transducer which has a direct FM output on one of the I.R.I.G. channels.

The temperature-sensing thermistor forms one arm of an essentially equal arm Wheatstone Bridge which is linear to ± 1% for a temperature deviation of ± 8°C from the balance point of the bridge. The bridge output is fed to a preamplifier with a nominal gain of 20 and then to a second amplifier (nominal gain 1.4 to 2.8) for the temperature signal output. The pre-amplifier output is also fed to a differentiator circuit which produces the signal that is later interpreted as the vertical component of the temperature gradient. The differentiator has a high frequency rolloff consisting of two R-C filters with 3 db points at 64 and 79 Hertz, respectively. The differentiator has a nominal gain at 1 Hertz of 18.47 based on the circuit parameters; the measured value is 18.39. Frequency response is -3 db relative to a differentiation at 44 Hz (measured and calculated).

The response of the thermistors is discussed in the paper by Lueck, Hertzman and Osborn (1977). Calibration of the thermistors consists of measuring the resistance at one or more temperatures that are in turn measured by a mercury-in-glass thermometer. To date no concerted effort has been made to ensure or enhance the accuracy of the temperature measurements. The relative temperature measurements are probably within ± .1°C, or better, depending on the number of calibration points. But the absolute accuracy requires calibration against an STD trace to be within ± .2°C. On the Azores and Bermuda cruises there were oscillations in the temperature gradient data, and to a lesser extent in the electrical conductivity gradient. It has not been possible to locate the source of the problem, since on test cruises in local waters the problem cannot be produced. Hence, it may be some interaction of the ships with the instrument, or some unknown difference in procedure at the two locations which is causing the problem.

The pressure is measured with a Vibrotron pressure transducer that is calibrated with an Amthor model #452 dead weight tester. The transducer is driven by a United Controls Amplifier. The accuracy and interpretation of the pressure record is discussed in the section dealing with the fall speed of the instrument body.

The electronics associated with the velocity probe are covered extensively in the paper by Osborn and Crawford (1977). The output of electrical conductivity is treated in a similar fashion to the output of the temperature preamplifier, the signal and its time derivative are both telemetered to the surface. The details of the circuit and its operation will not be discussed in this paper because the data have not yet been systematically analyzed.

C Data telemetry

Data from these instruments are converted from a time varying voltage to a frequency modulated (f.m.) signal by voltage controlled oscillators (vco's) inside the pressure case. The output of the different oscillators is summed by an operational amplifier and this signal is transformer-coupled to the wire link. On board ship, another operational amplifier

serves as a high impedance load on the wire. It outputs the signal both to an HP 3960B tape recorder for later analysis and to a set of SONEX S-35 discriminators and a chart recorder for real time data display. Fig. 6 is derived from Sippican Development Report R-621 and shows the attenuation as a function of frequency as the wire is unspooled in the water. Our configuration is slightly different, as one spool of wire is always in the water. The XWLs in use are 5000 feet long with 1500 feet on the source spool and 3500 feet on the shipboard spool. For deep drops - operations down to 800 metres - the spools have been interchanged with good success. The attenuation of the signal is a problem, especially the differential attenuation with frequency as a function of frequencies. We have used the I.R.I.G. ± 7.5% deviation channels with center frequencies as low as .73 kHz and as high as 10.5 kHz (see Table I). The attenuation is compensated for by increasing the gain of the shipboard operational amplifier which loads the XWL. The differential attenuation is counteracted by setting the vco's up with tapered output amplitudes. Thus the highest frequency has the largest amplitude at the surface. As the instrument sinks, the differential attenuation reverses the relationship and the low frequencies have the largest amplitude. Fortunately, the discriminators can accept a large range of input amplitudes (5 volts to 5 millivolts rms). Also, the highest frequency is the Vibrotron pressure gauge and if these data are lost at great depth we can approximate the depth from the last known value and the fall speed.

This telemetering system has worked well. There is the occasional aggravation of a broken wire at the surface or at depth. In high current or windy regions there is the problem of the surface wire running out before the instrument starts to return. The advantages of real time display and the ability to recycle without opening the pressure case to change tapes have been appreciated. As mentioned earlier, the Camel was lost once for two days by a release failure which caused it to stick in the bottom of a local inlet. The real time display allowed the observers to tell that it had hit bottom but that the case was not flooded. Hence, when it did not come up long after the salt blocks had dissolved, the crew knew it was worth trying to recover and made arrangements for a small submersible. Fortunately, the tidal currents (or just time and the buoyancy)

broke it loose. The instrument has also come to rest on the halocline in the local inlets where $\Delta S = 20\,‰$. Since the telemetry identifies this problem, the crew can wait, without worrying, for the salt blocks to dissolve.

Table 1 gives the vco center frequencies and the band width for ½ db attenuation. The 14.5 kHz channel is used for tape speed compensation (TSC) and is recorded by itself on a separate channel at the tape recorder. Some of the Vibrotron pressure transducers are on the 14.5 kHz channel. In these cases we divided their frequency by two inside the instrument and used the 7.5 kHz data channel. Upon playback the TSC signal is fed to a special discriminator which automatically feeds a correction signal to the data discriminators to correct for fluctuations in the tape speed. The TSC signal is put on a separate channel so that the levels of the f.m. data signal can be adjusted using the recorder's input meter. The noise seems to be lower if the two signals are fed to the discriminator set separately.

Calibration of the oscillators and discriminators is performed with a digital multimeter (Fluke 1000A or Dana 3800A), a counter (HP523CR) and a Wave-Tek oscillator. The center of the band is adjusted to 0 volts and one band edge set to ± 1.414 volts at ± 7.5% deviation for the discriminator, or ± 7.5% deviation at ± 2.5 v for the oscillators. The other band edge is then checked and recorded. For digitization of the data, the IOUBC PDP-12 computer contains a 10-bit digitizer. It was augmented in January 1977 by a 12-bit unit which will be used henceforth.

D Fall speed of the Camel

The pressure gauge in the instrument measures the pressure as a function of time. The data are stored on magnetic tape and digitized. For analysis, the data are digitized at a rate of 200 or 250 Hz, depending on the data set. This high rate is not needed for the pressure data, but the system is not designed to digitize different channels at different rates so the rate is determined by the highest rate required. The pressure data are then averaged in blocks of 128 points, then converted to pressure using

the calibration of the Vibrotron as determined in the laboratory with the dead weight tester. The calibration data are fitted with a cubic polynomial; that formula is used to convert the averaged values to pressure.

The mass of the instrument as launched is 75 ± 5 kg (corresponding to a weight of 740 ± 50 Newtons). After the instrument was dropped for the first time, *changes* in the mass became more important than the actual value. The buoyancy of the instrument is estimated by weighing the instrument in the water when fully prepared for a drop. Because of the motion caused by the small waves, the value is not very precise and the fine adjustment is done from the fall speed calculated from the pressure records. Experience gained by weighing the instruments just before release indicates that the fall speed is between .40 and .55 m/s when the instrument is ballasted to 18 to 27 Newtons heavy.

Measurements of the falling and rising speeds of the Camel taken during the field trip to the Azores can be used to estimate the drag coefficient, assuming the fall speed is quadratic in the excess weight and that the relationship is the same for a rising and falling instrument. On drops 5 and 6 the observed fall speeds were .53 and .51 m/s, respectively. The rise speeds are also available for portions of these two drops (.85 and .45 m/s, respectively). The difference is attributed to the fact that half of the release weight did not fall away immediately on drop 6. This drop is not the first time a weight failed to release, but perhaps failures occur more often than previously expected. For this pair of drops, the total drop weight is known to be 93.6 Newtons (21 lbs) when weighed in air, 85.3 Newtons in water. The following equations can be used to describe the system:

$$B = A\ (.85\ \text{m/s})^2 \qquad (1)$$

$$B - \frac{85.3}{2} = A\ (.45\ \text{m/s})^2 \qquad (2)$$

$$E = A\ (.52\ \text{m/s})^2 \qquad (3)$$

$$B + E = 85.3\ \text{Newtons} \qquad (4)$$

where B is the buoyancy of the instrument with both drop weights released, E is the excess weight when falling, A is the drag coefficient, and the average fall speed is taken to be .52 m/s. We have more than sufficient

equations for a solution which is :

A_1 = 86 Newtons/m^2/s^2 A_2 = 92 Newtons/m^2/s^2

B = 62 Newtons

E = 23 Newtons

where A_1 is derived from equations 1, 3 and 4, while A_2 is derived from equations 1 and 2. These values are in general agreement with a few crude measurements of excess weight derived with a small hand-held scale in sheltered portions of a local inlet.

The resultant profiles of depth as a function of time are plotted on 30-inch paper at scales of 25 m/inch and 16 s/inch. The slope of the line is the fall speed. In addition to the plot, the data are fitted to a series of linear polynomials using 16 values for the depth, each separated by .64 or .512 seconds (depending on the digitization rate). These depths correspond to the interval over which the velocity data are analyzed to estimate the local rate of energy dissipation. These estimates of the fall speed scatter quite a bit about the mean. Table II shows the computer printout for drop 15 in the Azores. The first column is the depth, the second column is the fall speed estimated for the linear fit to 16 successive values of the depth averaged over .64 seconds, the third column is the sum of the fall speed values and the last column is the average fall speed up to that point. It should be remarked that the depth of release is always the surface but sometimes the calculated depth can vary by several metres due to discriminator calibration, transducer hysteresis and/or temperature effects. Starting the first drop of the day, the instrument is at ship laboratory temperature; the temperature decreases for later drops. One can see the scatter, such as the low values of .49 m/s at 179 m and 562 m. These low values are probably due to noise combined with the least count problems with the digitizer. The least count on the digitizer corresponds to approximately .94 m, so the whole time interval of 10.24 seconds corresponds to about 5 m or 5.3 counts. The last bit on the digitizer has been found to have a favored value (there is a 2 to 1 preference in the least significant bit, Crawford, personal communication). The slope of the line fitted by eye, between 50 m and 380 m depth, is 52.5 cm/s. The average of the estimated velocities eliminating the first three and last value (instrument may

have been accelerating during those intervals) is 52.14 cm/s. The average fall speed derived from dividing the change in depth by the time from the fourth depth to the second from last depth is 52.05 cm/s. The average from 60 m depth to 737 m depth is 51.98 cm/s. The value used for the dissipation calculations was 52 cm/s based on the fact that the depth versus time curve showed some curvature above the 50 m depth.

In order to study the fall speed variation with depth, the depth versus time record for this drop was fitted using a cubic spline routine available on the UBC computer. Essentially, the fit produced has the minimum curvature possible within the allowed variation for each individual point and the profile as a whole. For more details on the technique see Reinsch (1967). The results are given in Table III which show the fitted depth, the slope of the fit (fall speed), and the curvature of the fit (acceleration). There is a minimum in the fall speed around 480 m depth which may be real or a problem with the calibration values which show a peculiar minimum in slope in the 600-700 psi region (Table IVa, b). It seems that .52 m/s is a reasonable estimate of the average fall speed and the error is $\sim \pm$ 10 mm/s or $\pm$ 2%. Table III suggests the error could be decreased significantly by adding a linear variation with depth to the fall speed. It is unclear how much of the deeper variation is due to the instrumentation and how much is real.

The error in fall speed contains two parts, the error in the pressure measurement by the Vibrotron and the errors associated with the differencing of the presure. The errors in the pressure measurement that are constant with depth do not influence the fall speed calculation. It is the depth- or time-variable errors that are important. One source of error is the temperature sensitivity of the resonant frequency of the Vibrotron pressure transducer. Calibrations of the transducer at 19.8°C and 13°C showed the transducer used in the Azores and the Bermuda cruises to be much more temperature sensitive at low pressures than at higher pressures. Table IVc shows the difference in the measured frequency between the two temperatures. The difference in measured frequency shows a consistent trend, with fluctuations that may be associated with the errors in the calibration technique being amplified by the differencing of the values.

A change of three Hertz corresponds to about a 1 m depth increment so the effect over the whole water column is about 2 m in 600 m, or less than .5%. The change in sensitivity with temperature is most pronounced near the surface. If we consider the first 50 psi of change we have .5 m in about 30 m or .23%/C°.

The different methods for calculating the *average* fall speed from the pressure data all give answers that are within 1% of the value chosen for the mean fall speed over the drop. If one excludes the calculation based on lines drawn by eye, the disagreement is less than .5% over the whole drop. The small-scale variability of the fall speed cannot be examined to this accuracy, of course, because of the least count error problem of the digitizer discussed earlier.

There remains the question of stability of the fall speed with depth. What is the length of time, or the depth to which the instrument has sunk, before the fall speed has reached its terminal value? What are the variations with depth after 'terminal velocity' is reached?

The stability of the fall speed has been examined for a drop in a local fjord, Howe Sound. For this drop a 0-500 psi pressure gauge was installed for greater resolution of the depth trace. The initial speed (.54 m/s) was 97.3% of the terminal value (Table V). The fall speed reaches 98% of its terminal value of .555 m/s (the average of .553 and .557 m/s) at a depth of 40 m. This depth is greater than that required for the data collected along the Atlantic Equatorial Undercurrent wherein all the drops that were analyzed by Crawford (1976), except for one, reached their terminal velocity by 15 to 20 m depth. The data collected in the Azores show terminal velocity is achieved by 20 m in all but one of the drops which required 29 m to reach the terminal value. The solution to the terminal velocity question requires drops with a pressure transducer with a limited full-scale range, or else an internal recording system of great resolution such as developed by Cox for their free-fall system. These drops will give the resolution in pressure necessary to look at variations in its first derivative, which is the fall speed. Our interest to date has been on the deeper part of the water column, below the first 10 to 20 m

in general, so that the speed-up at the start has not been a problem. For the portion of this Howe Sound drop below 75 m, the fall speed is constant to an accuracy of 0.4%.

Some of the fall speeds measured on the Bermuda cruise show an increase in speed of .05 to .10 m/s with depth for the first 15 to 40 m (Gargett, personal communication). This extreme situation is not seen in the other cruises' data; it remains unexplained. One possible cause could be an air bubble trapped in the salinometer system bellows. The instrument design is such as to make this quite possible. This bubble would compress with depth, thereby decreasing the buoyancy and allowing the fall speed to increase. The effect is the opposite of that due to an increase in the density of the water. The estimation of the volume of air necessary must be crude because of the imprecise knowledge of the excess weight on the body as a function of the fall speed. However, the earlier results suggest a value of .5 litre or less. Data analysis for the Bermuda cruise was also complicated by the fact that below a certain depth the pressure signal faded out, so that greater depths had to be estimated from the last known pressure and the fall speed. The loss of pressure signal was not a problem previously, although it had the highest center frequency, and was attenuated most by the transmission system. The pressure transducer has now been overstressed by operating 25% beyond its full scale and shows a tendency to oscillate unstably at high pressures and low temperatures ($\theta < 13°C$). Thus, there may be a decrease in amplitude with decreasing temperature.

E Motion of the Camel

Since the Camel is being used to support the velocity probe, it is important to investigate the possible effects of body motions of the vehicle on the velocity measurements of the probe. There are two aspects to this problem. First, consider the probe so that its operating principles can be understood. As described in Osborn and Crawford (1977), the probe is a symmetric airfoil of revolution whose axis is aligned with the axis of the Camel. As the probe moves through the water, the mean velocity vector of the water is axially along the probe, i.e. the velocity vector has zero angle of attack relative to the probe (axis). Any horizontal velocity component in the water relative to the probe leads to a non-zero angle of attack for the total velocity vector, hence a transverse force is exerted on the probe tip. The two perpendicular components of this transverse force are sensed by two perpendicular piezoceramic transducers inside the probe and the force components are converted to electrical signals. The output of the probe is linear in the cross-stream velocity (U) and the axial velocity (V),

$$\text{Output} = \frac{1}{2}\rho S U V$$

where ρ is the density and S is the sensitivity. Fluctuations in the mean fall speed of the Camel (which could be considered fluctuations in the mechanical gain of the system) have already been considered. Fluctuations in the cross stream and the axial velocity due to pendulum-like oscillations of the body about its vertical axis will now be considered. After that there will be discussions of constraints due to the probe's limitation that the total angle of attack be less than some maximum critical angle between 10° and 15°.

Measurements of the instrument, ballasted for neutral buoyancy, show the natural period of oscillation to be 7 seconds with the motion highly damped. Comparing this value to the theoretical calculation based on the known parameters, one can check his understanding of the situation.

The question of natural frequency of oscillation can be looked at by estimating the oscillation period of the instrument as a pendulum

$$\omega = \sqrt{wh/I} \qquad \sqrt{\frac{mg \cdot h}{\ell^2/12}} \qquad \sqrt{\frac{12gh}{\ell^2}}$$

$$T = 2\frac{\pi}{\omega} = 2\pi\ell/\sqrt{12gh} = \frac{2\pi \cdot 4.2\text{m}}{\sqrt{12 \cdot 9.8\text{m/s} \cdot 47\text{m}}} = 3.6 \text{ s}$$

where w is the weight, h the metacentric height, I the moment of inertia, and ℓ the length. Since the instrument is in water, the effect of the virtual mass should be included. The virtual mass is the water associated with the cylinder which must move at the same time. The effect is to increase the moment of inertia. For a long prolate spheroid, the added mass is equal to the displaced mass (Lamb 1945) so the period would increase by a factor $\sqrt{2}$, to 5 s. An accelerometer could have been installed to measure this effect, but since the frequency is below the range of interest we did not feel the expense was warranted. As a further check we must see if the magnitude of the tilt is significant for the interpretation of the data.

For a consideration of the effect of possible tipping of the instrument due to the shear in the water, the velocity data collected by Bruce and Katz (1975) along the Atlantic Equatorial Undercurrent can be used. The largest value of the mean shear over a vertical distance of 10 m is .06 s^{-1}. The mean horizontal acceleration of the Camel, assuming some point on the body remains at rest with the local water column, is

$$a = \frac{\partial u}{\partial t} = \frac{\partial u}{\partial z} \cdot \frac{\partial z}{\partial t} = .06 \cdot v_{fall} \cong .03 \text{ m/s}^2 ,$$

the force associated with such an acceleration is

$$F = ma = 75 \text{ kg} \cdot .03 \text{ m/s}^2 = 2.3 \text{ Newtons} .$$

This force can come from two possible sources. Firstly, the aerodynamic lift force on the tapered lower end of the cylinder, and secondly the cross stream drag force on the cylinder as a whole. The aerodynamic lift force due to the potential flow, after Allen and Perkins (1951), is :

$$F_1 = \rho AVu.$$

A is the cross-sectional area of the body, V is the axial speed, and u is the local cross-stream speed. The force, F, acts at the position of

changing cross-sectional area, i.e. the ends of the instrument. From the same source the force due to flow separation is:

$$F_2 = \int \tfrac{1}{2} \rho u^2 (C_{d\alpha=90^\circ}) 2r \, d\ell \ .$$

$C_{d\alpha=90^\circ}$ is the drag coefficient for a cylinder perpendicular to the flow and r is the radius. This force acts all along the body at the lower end where C_d is probably reduced due to the axial velocity and the close proximity of the upstream end of the cylinder, which diminish the effect of flow separation. In order to estimate the magnitude of these forces, one must first estimate the local cross-stream velocity as a function of position along the cylinder. A reasonable estimate can be derived by assuming the brushes are at rest with respect to the local water velocity. One further assumption is to ignore the forces on the portion of the body above the brushes. Since that portion of the instrument is in the wake of the brushes it is inappropriate to use a potential flow theory to calculate an aerodynamic lift force. The effect of the u^2 drag is limited since the region is close to the brushes and the speed u increases linearly with distance from the point of zero relative velocity. The distance from the brushes to the nose is 3.3 m.

$$F_1 = \rho A v u = 1000 \frac{\text{kg}}{\text{m}^3} \cdot 2.2 \times 10^{-2} \text{m}^2 \cdot \frac{.5 \text{ m}}{\text{s}} \cdot .06 \text{ s}^{-1} \cdot 3.3 \text{ m}$$

$$= 2.2 \text{ Newtons}$$

which is a sufficient force to provide the acceleration required for some point on the body to 'keep up' with increasing horizontal speed. The torque exerted by this force about the C of M is

$$M_1 = (2.2 \text{ Newtons}) \ 2.2 \text{ m} = 4.8 \text{ Newton-metres.}$$

For the cross-stream drag force we integrate down to, but not including the nose

$$F_2 = \int_0^{3\text{m}} \tfrac{1}{2} \cdot 1000 \frac{\text{kg}}{m^3} \cdot (.06 \cdot \ell \text{ s}^{-1})^2 \ 1.2 \cdot .17 \text{ m} \, d\ell$$

$$= \tfrac{1}{2} \cdot 1000 \cdot 3.6 \times 10^{-3} \text{ s}^{-2} \cdot 1.2 \cdot .17 \text{ m} \frac{(3\text{m})^3}{3}$$

$$= 3.3 \text{ Newtons}$$

Again, this is more than enough force to provide the horizontal acceleration.

The torque about the level of the brushes is

$$M_2' = \int_0^{3m} F_2(\ell)d\ell = 3/4 \cdot 3m \cdot F_2 = 7.43 \text{ Newton-metres.}$$

This torque can be transferred to the center of mass by subtracting F_2 times the distance between the brushes and the center of mass (1.6 m). So the torque about the center of mass due to the u^2 force is

$$M_2 = M_2' - F_2 \cdot 1.6 \text{ m} = 2.15 \text{ Newton-metres}$$

The total torque ($M_1 + M_2$) is 7 Newton-metres. What is the angle of tilt? The center of mass is .5 m below the center of buoyancy; equating the torque from the forces to the torque due to the stability of the instrument gives

$$7 \text{ Newton-metres} = 740 \text{ Newtons} \cdot .5 \text{ m} \cdot \sin\theta \rightarrow \theta = 1.1°$$

This is probably an overestimate of the tip because the total force is three times that necessary to produce the horizontal acceleration. An estimate for the point of zero velocity 1 m lower would produce.

$$F\ (2 \text{ m}) = \left(\frac{2.3}{3.3}\right) F_1 = 1.53 \text{ Newtons}$$

$$M_1(2 \text{ m}) = \left(\frac{2.3}{3.3}\right)^2 M_1 = 2.3 \text{ Newton-metres}$$

$$F_2(2 \text{ m}) = \left(\frac{2}{3}\right)^3 F_2\ (3 \text{ m}) = 1 \text{ Newton}$$

$$M_2'(2 \text{ m}) = \left(\frac{2}{3}\right)^4 M_2\ (3 \text{ m}) - .6 \text{ m} \quad (2 \text{ m}) = .9 \text{ Newton-metres}$$

Now, the assumption that F_2' and M_2' can be calculated without including the contributions from the regions above the point of zero velocity relative to the local water, becomes more suspect. In fact, one might argue that a) F_2' 0 since we are now near the center of the body and the force distribution is symmetric, and that b) M_2' should be doubled to 1.8 Newtons. The role of the brushes in the lateral force balance is difficult to assess. Their diameter is comparable to the cylinder but their projected area when viewed from the side is equivalent to .3 m length of the tube. They are designed to be effective drag elements in the vertical direction and not the horizontal. For a torque of 3.3 Newton-metres, the tip of the instrument is

$$\theta = .51°$$

Hence, we can conclude that the tipping of the instrument is probably restricted to less than 1°, even in the presence of fairly strong values of the local velocity shear.

There is another much more serious aspect of the problem: that is, the question of the mean angle of attack of the total velocity vector. The problem arises because the velocity sensor used is a lift force sensor (see Osborn and Crawford 1977) and has a maximum angle of attack limitation somewhere in the 10° to 15° range. For the data collected at the equator, the fall speed of the instrument was in the 40 to 45 cm/s range. If the length scale for the distance between the nose probe and the point at rest with respect to the local water is 2 metres, then the relative horizontal velocity at the nose is

$$u = 2 \text{ metres} \cdot \frac{\partial u}{\partial z} = 12 \text{ cm/s}$$

for a large value of $\frac{\partial u}{\partial z} = .06 \text{ s}^{-1}$. The mean angle of attack is then

$$\frac{12 \text{ cm/s}}{40 \text{ cm/s}} = \tan \alpha \rightarrow \alpha = 16.7°$$

Thus, the maximum angle of attack is almost certainly exceeded. The problem of large mean shears is much more serious when viewed in this context rather than in the context of the tipping problem. The easiest solution is to increase the fall speed, thereby reducing the angle of attack. Since the force producing the horizontal acceleration of the body is the aerodynamic lift force, which is linear in the fall speed, the body will continue to track the horizontal motion. The tipping will increase with speed since the dominant contributor to the torque is the lift force. Hence, there is some middle ground where the relative effects cross over and an increase in speed is no longer any help. Removing the present salinometer and returning to the earlier configurations would bring the probe closer to the point of no relative motion, without significantly reducing the static stability. This would reduce the effect of a large mean shear.

There is another aspect to this problem: the contamination of the measured velocity spectrum by vibrations. The details of this contamination are covered in Osborn and Crawford. It is sufficient for the discussion at hand

to say that the turbulence signal is presently (v_{fall} = 40 to 55 cm/s) in a lower frequency region of the spectrum than the contamination due to vibrations. Increasing the fall speed linearly increases the apparent frequency of the turbulence signals and unless steps are taken to avoid trouble, the desired data can become contaminated by the unwanted vibration signal. The Camel was not designed with the vibration problem in mind. Some of the sources of noise have been reduced or eliminated (stiffening has doubled some resonant frequencies). The best solution is to be aware of the problem at the initial design stage and avoid shapes that are prone to vibration, such as the weights at the end of rods. The thermistor mount, the weight holders, and the salinometer system are major sources of noise in the present design.

The rotation orientation of the Camel is measured with a flux gate compass purchased from Mr Neil Brown, who calibrated it at 2° intervals. The instrument was installed in the Camel to make sure the rotation of the body was slow enough that velocity signals were not being adversely affected. The period of rotation is generally greater than 200 seconds. Nothing was designed into the instrument to make it rotate, and no effort was exerted to stop this slow rotation. Some changes in rotation are seen at the equator when the instrument enters the high shear region at the top of the undercurrent. Data show variations that range from a tripling of the rate of rotation in the same direction, to a stopping of the rotation and even a reversal.

F Suggested improvements to the Camel design

Based on our experiences with the Camel and its data, the following improvements seem appropriate:

1. A free-fall vehicle for velocity shear profiling with the airfoil probe should fall faster than .5 m/s in order to reduce the chance of excessive mean angles of attack. The vibration problem will probably limit the maximum fall speed of the instrument to something on the order of 1 m/s.
2. Shorten the instrument by removing the mechanical parts for the salinometer (remove entirely or put the bellows, etc., on the other end) and shortening the pressure housing. This reduction in length will also reduce the mean angle of attack seen by the probe in regions of high shear in the ocean.

3. The fall speed should be measured more accurately, perhaps with a Paros Scientific pressure transducer with appropriate data storage or transmission system. Professor J Smith at the University of Washington has some small-ducted current meters that are probably quite suitable for a direct measurement. Either approach would reduce the error in the fall speed by at least a factor of 2, as well as give a much better idea of the variations of fall speed with depth.

4. Accelerometers for measuring tilt and vibration of the body should be included in the next instrument to document tilts and vibrations directly.

V Pumpkins

Work with the early instruments at the University of British Columbia indicated a need for a set of small, simple instruments to separate the temporal variations of the microstructure fluctuations from the spatial variations. The first instruments had a 'turn around time' on the order of ½ hour between successive drops. A series of drops with one of these instruments was very interesting but it was very difficult to relate fluctuations between profiles. What was needed was a set of instruments that could be dropped simultaneously with a given spatial separation or at different times in the same location. To be useful such a set of instruments should be simple, so that the chances are high that all of them will operate at once. The design problem reduces to the question of what is the 'minimum' instrument necessary to make useful microstructure measurements.

The decision was made to measure the microstructure and not just the fine structure as done by the simple instrument described by Osborn and Cox (1972) and Hacker (1973). The problem under investigation was: What are the time and space scales of thermal microstructure? An initial attempt was made to develop an instrument that telemetered the data up an XWL as a low-frequency signal. The electronics in the probe consisted of a bridge and a differentiator, the outputs were added together and applied to the wire link. At the upper surface a set of electronics interpreted the low-frequency fluctuations and drift as the temperature profile and the high-frequency fluctuations as the temperature derivative. While the system could be made to function in the laboratory, it never showed any signs of working in the field. The major problem was noise picked up by the wire link functioning as an antenna. On one trial, this instrument was lost (it is the only free-fall instrument still unrecovered) and the approach was abandoned. The decision was to make a set of electronics that measured temperature and temperature gradient and telemetered the data to the surface using two of the I.R.I.G. FM channels. The circuit is essentially the same as the Camel, except for the gains and the fact that the bridge is not operated in an equal arm balanced configuration. Thus, the output of the temperature channel is not a linear function of the

temperature. The advantage is that the gain of the temperature channel is greater by a factor approaching 2 for the same voltage across the thermistor gradient. The Camel was operated in a configuration like this for local development work because the water is uniform to within just a few degrees below the thermocline. Therefore, more gain was important and the poorer linearity was not a problem because the range was not as large as that seen in the open ocean. Power for the electronics is provided by four Eveready 216 (NEDA 1604) batteries. These are non-rechargeable alkaline cells.

Figure 7 shows a schematic drawing of one of the three Pumpkins that were built and operated. The flotation is provided by a Viny 103-12 plastic float. The instrument is designed so that even if the instrument housing floods there will be enough buoyancy (once the weights are released) to return the entire instrument to the surface.

The instrument consists of a float, a set of wings and a pressure case for the electronics. There is an OAR citizen's band radio transmitter on the upper end for location on the surface. The wire link spool is mounted next to the radio, while an empty spool is mounted on the other side of the radio to provide symmetry. The wings are from sonobuoys and can fold down about 45° for easier handling on deck. The release is a stretched pin Richardson-type, made of aluminum rather than the stainless steel used on the Camel. The acoustic pinger is a disposable model. The pressure case is made of stainless steel arc welded together with an O-ring seal for the endcap. Steel was chosen for the pressure case because of fear of damage to an aluminum case. The connection to the thermistor is via an Electro-Oceanics bulkhead connector. The composite output telemetry signal is taken through the case with an Electro-Oceanics penetrator. The thermistor is soldered to an Electro-Oceanics male connector and the joint is epoxy encapsulated. The plug is mounted in the tube on the lower endcap and the connector inserted into the bulkhead connector. The design we had was inconvenient to mount and required the connector and thermistor to be potted together, which was a time-consuming operation.

The electronics for the Pumpkins does not include a pressure transducer because of the restricted room in the pressure case and the desire to avoid the complexity of the added circuitry. Instead, there was one circuit made that consisted of a Vibrotron pressure transducer and a rotation rate circuit - a coil wrapped around a permeable iron core. Drops made with this electronics are used to estimate the fall speed as a function of added weight. The final estimate of the fall speed is made by fitting the temperature profile measured by the Pumpkin against that measured with an STD. Remember the object of the study is to look at the horizontal extent of the microstructure patches so the exact depth is not crucial.

There is one unanticipated operational problem that arose from this design. During drops along the equator in the Atlantic Ocean, the current shear was so great that the fine copper wire from the XWLs was pulled sideways and the rotation of the Pumpkin wrapped the wire around the radio antenna, leading to premature breakage. This problem was solved by the addition of a loop at the top of the radio antenna to guide the wire safely above the aerial.

The fall rate and rotation rate of the Pumpkins as measured at the equator in the Atlantic are summarized in Table VI. The rotation rate values are derived from analysis of the analog data telemetered up the wire. A more detailed digital analysis of the pressure data, including a spline fit as described earlier, was performed to calculate the fall speeds. Only one drop with each instrument using the pressure measuring electronics was performed along the equator.

References

Allen, H J and E W Perkins (1951) A study of effects of flow over slender inclined bodies of revolution. National Advisory Council for Aeronautics Report No. 1048.

Brown, J F and C S Cox (1973) Design of light, cylindrical pressure cases. Engineering Journal 35-37.

Bruce, J G and E J Katz (1976) Observations in the Equatorial Atlantic during GATE, June and July 1974 from Atlantis II. Woods Hole Oceanographic Institution Technical Report 76-54, 90 pp.

Caldwell, D R, S D Wilcox and M Matsler (1975) A relatively simple freely-falling probe for small-scale temperature gradients. Limnology and Oceanography 20, 1035-1042.

Crawford, W R (1976) Turbulent energy dissipation in the Atlantic Equatorial Undercurrent. Ph.D. Thesis, Institute of Oceanography, University of British Columbia, 149 pp.

Drinkwater, K F (1973) The role of tidal mixing in Rupert and Holberg Inlets. M.Sc. Thesis, Institute of Oceanography, University of British Columbia, 58 pp.

Elliott, J A and N S Oakey (1976) Spectrum of small-scale oceanic temperature gradients. JFRBC 33: 10, 2296-2306.

Galloway, J L (1974) Prototype of a continental shelf tide gauge. M.A.Sc. Thesis, Dept. of Electrical Engineering, Faculty of Applied Sciences, University of British Columbia, 73 pp.

Gregg, M C and C S Cox (1971) Measurements of oceanic microstructure of temperature and electrical conductivity. Deep-Sea Research 18, 925-934.

Hacker, P W (1973) The mixing of heat deduced from temperature fine structure measurements in the Pacific Ocean and Lake Tahoe. Ph.D. Dissertation, University of California, San Diego, 121 pp.

Lamb, H (1945) *Hydrodynamics*, 6th Ed., Dover Publications, New York, N.Y.

Lueck, R G, O Hertzman and T R Osborn (1977) The spectral response of thermistors. In press, Deep-Sea Res.

Mortensen, A C and R E Lange (1976) Design considerations of wing stabilized free-fall vehicles. Deep-Sea Res. 23, 1231-1240.

Oakey, N S (1977) An instrument to measure oceanic turbulence and microstructure. BIO Report Series/BI-R-77-3/May 1977.

Osborn, T R (1973) Temperature microstructure in Powell Lake. J. Phys. Oceanogr. 3: 3, 302-307.

Osborn, T R (1974) Vertical profiling of velocity microstructure. J. Phys. Oceanogr. 4: 109-115.

Osborn, T R and C S Cox (1972) Oceanic Fine Structure. Geophys Fluid Dyn 3, 321-345.

Osborn, T R and W R Crawford (1977) Turbulent velocity measurements with an airfoil probe. NATO Advanced Study Institute on Instruments and Methods in Air-Sea Interaction.

Reinsch, C H (1967) Smoothing by spline functions. Num. Math. 10: 177-183.

Sanford, T B, R G Drever and J H Dunlap (1977) The design and performance of a free-fall electromagnetic velocity profiler (EMVP). In press, Deep-Sea Research.

Simpson, J H (1972) A free-fall probe for the measurement of velocity microstructure. Deep-Sea Res. 19: 331-336.

Williams, A J (1974) Latching hook for instrumental retrieval. Ocean Eng. 2: 275.

Williams, A J (1974) Free-sinking temperature and salinity profiler for ocean microstructure studies. IEEE International Conf. on Eng. in the Ocean Environment Record, Catalogue No. 74 CH0873-0 OCC 279-283.

APPENDIX I

First Instrument

Parameters measured:

1 Pressure
2 Nose temperature
3 Wing temperature
4 Nose temperature high pass filtered and amplified
5 Wing temperature high pass filtered and amplified

Sensors:

Pressure:

Vibrotron pressure gauge, BJ Electronics Serial No. 5811, 0-500 psi range

Temperature:

Veco Z41A40 .058 cm glass probe

Characteristics:

Fall speed:

Nominal 20-25 cm/s.

Rotation rate:

Nominal one revolution per nine seconds.

Second Instrument

Parameters measured:

1 Pressure
2 Nose temperature
3 Wing temperature
4 Nose temperature gradient
5 Wing temperature gradient
6 Electrical conductivity
7 Electrical conductivity gradient
8 Two horizontal velocity components
9 Time variation of the horizontal magnetic field component
10 Time variation of the vertical magnetic field

Sensors:

Pressure:

Vibrotron pressure gauge, no serial number. 0-300 psi range.
BJ electronics No. 4193 - 0-1000 psi

Temperature:

Thermistor Veco 43A401C microbead thermistor coated with .016 mm of paralene-C by Sippican; later Thermometics beads were used.

Electrical conductivity:

A series of inductive circuits and sensors were tried but none ever operated successfully. The circuitry was finally removed to concentrate on the velocity measurements.

Velocity:

Airfoil probes manufactured at IOUBC
See Osborn (1974) and Osborn & Crawford (1977) for details.

Characteristics:

Fall speed: nominal 20-25 cm/s.
Rotation rate: dependent on wings used; up to 27-second period

Third Instrument

'The Camel'

Parameters measured:

1 Pressure
2 Nose temperature
3 Nose temperature gradient
4 Electrical conductivity
5 Electrical conductivity gradient
6 Angular orientation of axis
7 Horizontal velocity fluctuations

Sensors:

1 Pressure: Vibrotron pressure gauges -
(a) 300 psi gauge with no serial number
(b) BJ Electronics, Serial No. 4193; 0-1000 psi range
(c) BJ Electronics, No. 5075; 0-500 psi range

2 Temperature: Microbeads manufactured by Thermometrics, Inc. - see 'Pumpkins' for details.

3 Electrical conductivity: Modified Gregg & Cox type salinometer

4 Angular orientation: Flux gate compass manufactured on special order by N Brown.

5 Velocity: Airfoil probes manufactured at IOUBC. See Osborn & Crawford (1977) for details.

Characteristics:

1 Fall speed, 40-55 cm/s.
2 Rotation period greater than 200 s.

Fourth Instrument

'The Pumpkins'

Parameters measured:

A For Data:
  1 Temperature
  2 Temperature gradient

B For Calibration:
  1 Pressure
  2 Rotation

Sensors:

Temperature:

Thermometrics microbead thermistors No. BB05PB853N/A4°C (special order) with .0007" paralene-C coating by Sippican.

Pressure:

Vibrotron pressure gauge BJ Electronics, Serial No. 4191, 0-1000 psi range.

Rotation:

Coil wrapped around a permeable iron core

Characteristics:

Fall speed: Nominal, 20 cm/s.

Rotation rate: Nominal, .2 Hz (see Table VI).

List of Figures

1 Schematic drawing of the first instrument
2 Schematic drawing of the second instrument in the configuration used during the development of the velocity probe
3 (a) Schematic drawing of the Camel before the inclusion of the salinometer mechanism
(b) Drawing of the Camel in its final configuration
4 Schematic drawing of the salinometer mechanism showing the large low pressure air reservoir with the piston, spring, and bellows
5 Block diagram of the Camel electronics
6 Attenuation of the XWL as a function of frequency and the amount of wire in the water
7 Schematic drawing for a Pumpkin

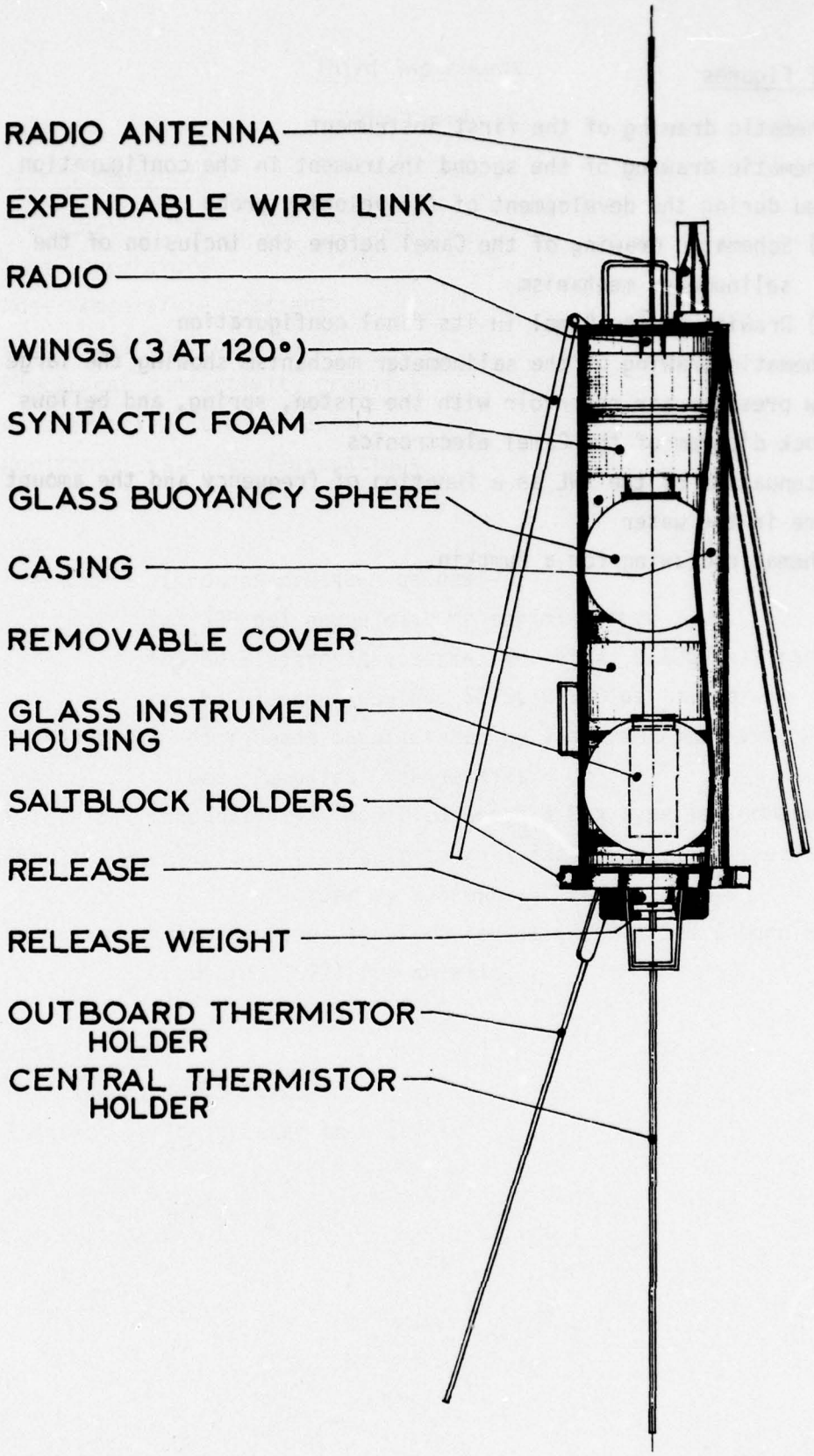
RADIO ANTENNA
EXPENDABLE WIRE LINK
RADIO
WINGS (3 AT 120°)
SYNTACTIC FOAM
GLASS BUOYANCY SPHERE
CASING
REMOVABLE COVER
GLASS INSTRUMENT HOUSING
SALTBLOCK HOLDERS
RELEASE
RELEASE WEIGHT
OUTBOARD THERMISTOR HOLDER
CENTRAL THERMISTOR HOLDER

Figure 1

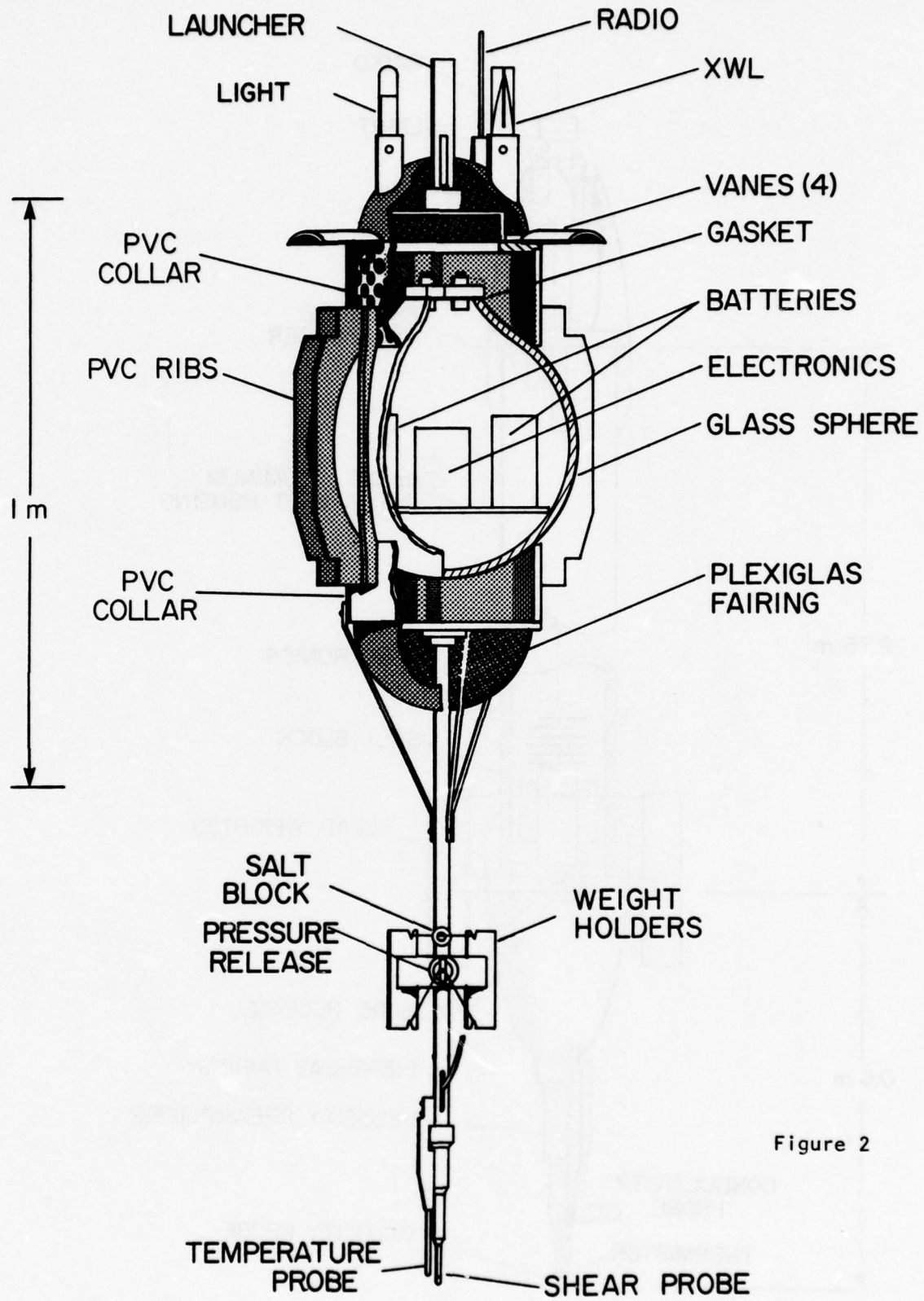
LAUNCHER
RADIO
LIGHT
XWL
VANES (4)
PVC
COLLAR
GASKET
BATTERIES
PVC RIBS
ELECTRONICS
GLASS SPHERE
1 m
PVC
COLLAR
PLEXIGLAS
FAIRING
SALT
BLOCK
WEIGHT
HOLDERS
PRESSURE
RELEASE
TEMPERATURE
PROBE
SHEAR PROBE

Figure 2

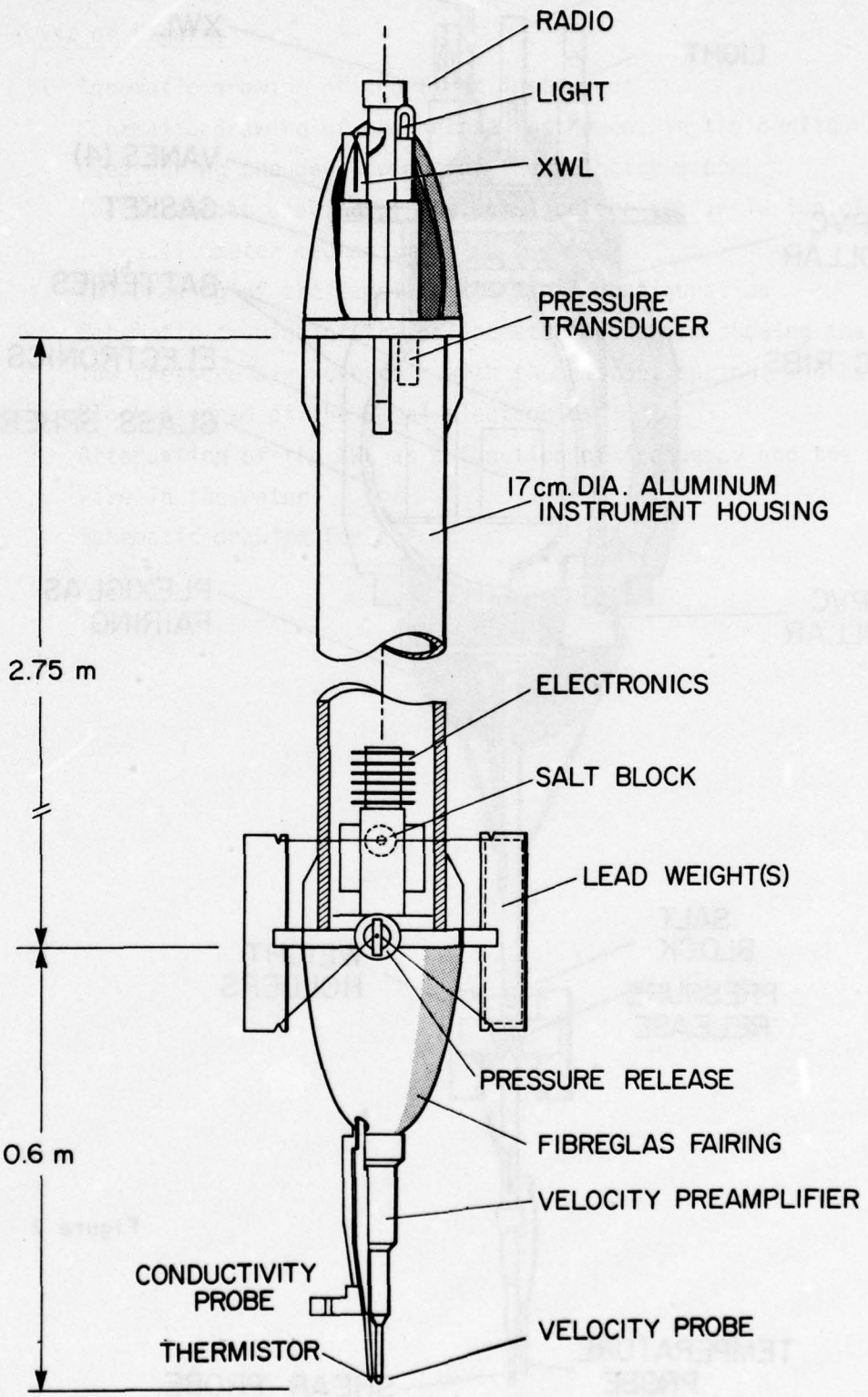
RADIO
LIGHT
XWL
PRESSURE TRANSDUCER
17cm. DIA. ALUMINUM INSTRUMENT HOUSING
2.75 m
ELECTRONICS
SALT BLOCK
LEAD WEIGHT(S)
PRESSURE RELEASE
FIBREGLAS FAIRING
0.6 m
VELOCITY PREAMPLIFIER
CONDUCTIVITY PROBE
VELOCITY PROBE
THERMISTOR

Figure 3a

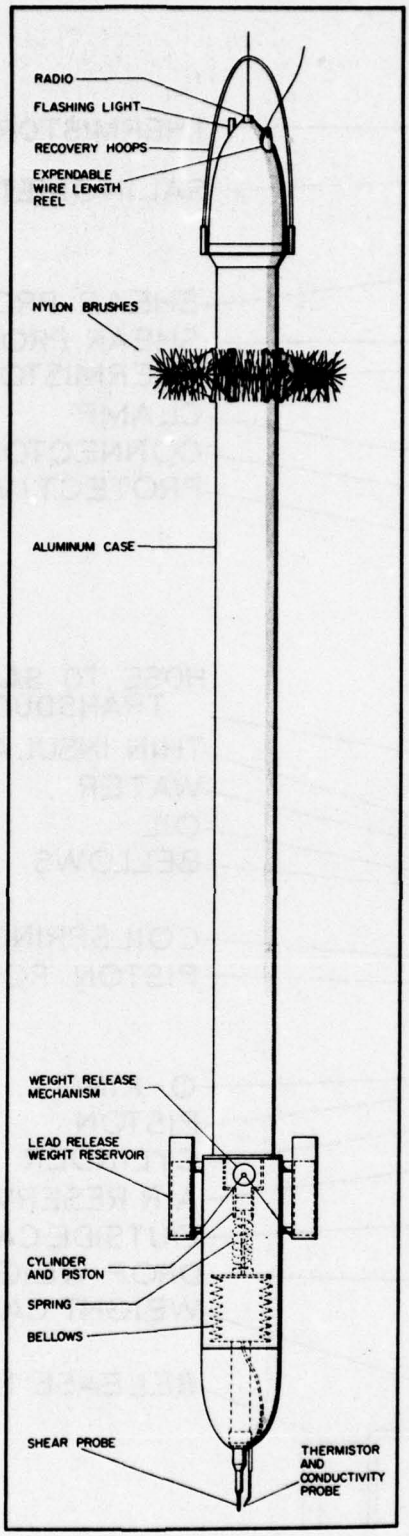
RADIO
FLASHING LIGHT
RECOVERY HOOPS
EXPENDABLE WIRE LENGTH REEL
NYLON BRUSHES
ALUMINUM CASE
WEIGHT RELEASE MECHANISM
LEAD RELEASE WEIGHT RESERVOIR
CYLINDER AND PISTON
SPRING
BELLOWS
SHEAR PROBE
THERMISTOR AND CONDUCTIVITY PROBE

Figure 3b

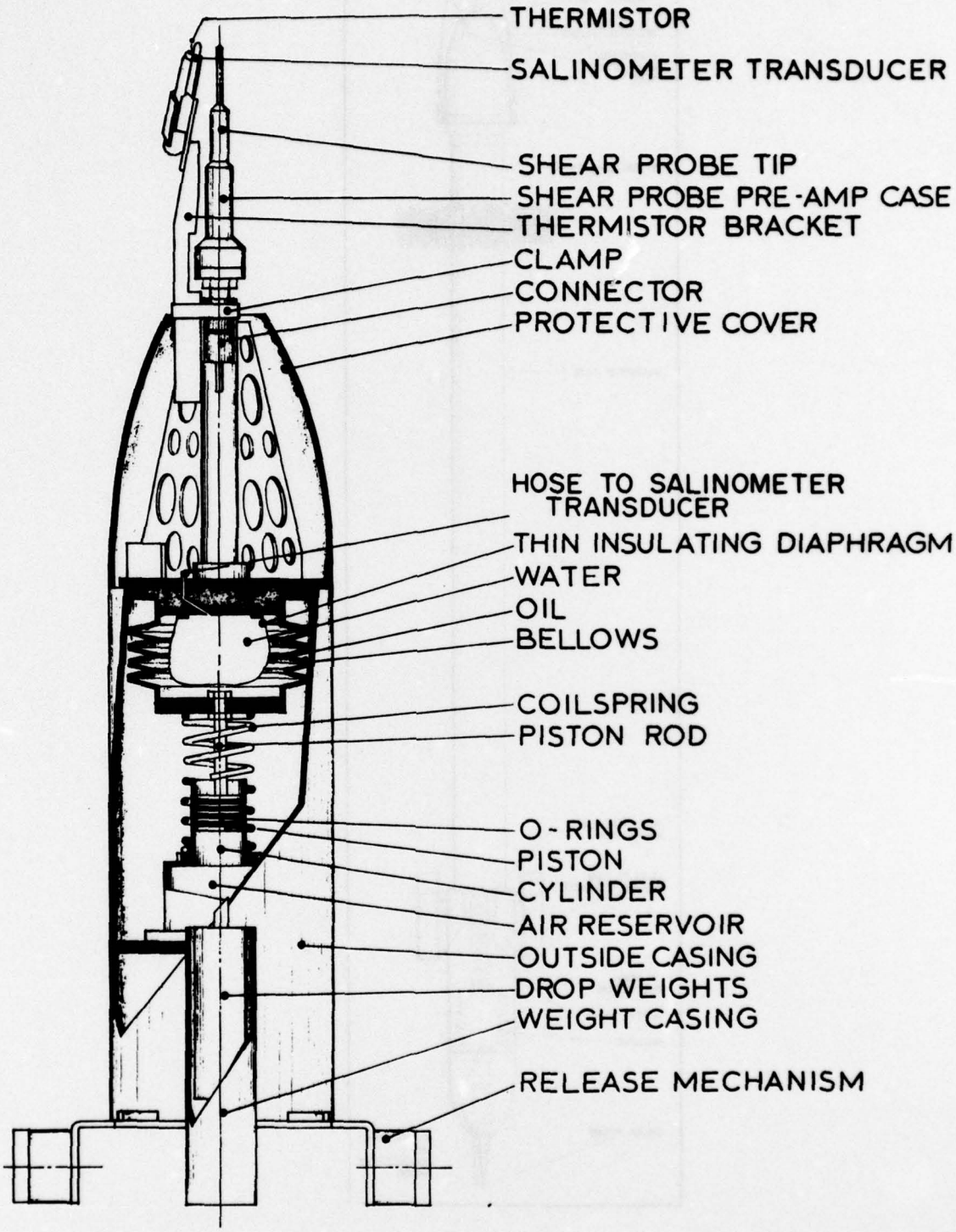
THERMISTOR
SALINOMETER TRANSDUCER
SHEAR PROBE TIP
SHEAR PROBE PRE-AMP CASE
THERMISTOR BRACKET
CLAMP
CONNECTOR
PROTECTIVE COVER
HOSE TO SALINOMETER TRANSDUCER
THIN INSULATING DIAPHRAGM
WATER
OIL
BELLOWS
COILSPRING
PISTON ROD
O-RINGS
PISTON
CYLINDER
AIR RESERVOIR
OUTSIDE CASING
DROP WEIGHTS
WEIGHT CASING
RELEASE MECHANISM

Figure 4

Figure 5

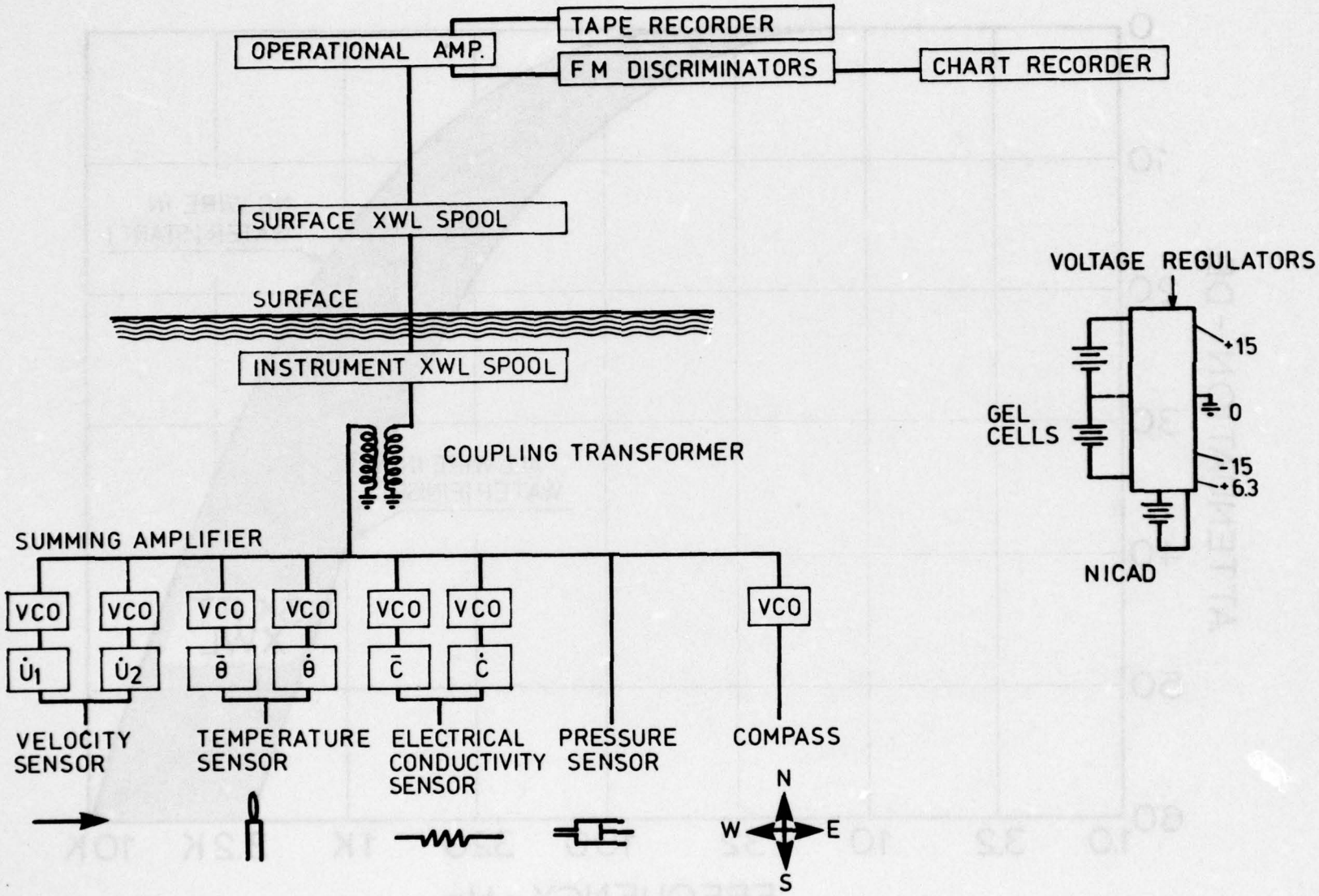
TAPE RECORDER
OPERATIONAL AMP.
F M DISCRIMINATORS
CHART RECORDER
SURFACE XWL SPOOL
SURFACE
INSTRUMENT XWL SPOOL
COUPLING TRANSFORMER
VOLTAGE REGULATORS
+15
0
-15
+6.3
GEL CELLS
NICAD
SUMMING AMPLIFIER
VCO
$\dot{U}_1$
$\dot{U}_2$
$\bar{\theta}$
$\dot{\theta}$
$\bar{C}$
$\dot{C}$
VELOCITY SENSOR
TEMPERATURE SENSOR
ELECTRICAL CONDUCTIVITY SENSOR
PRESSURE SENSOR
COMPASS
N
W
E
S

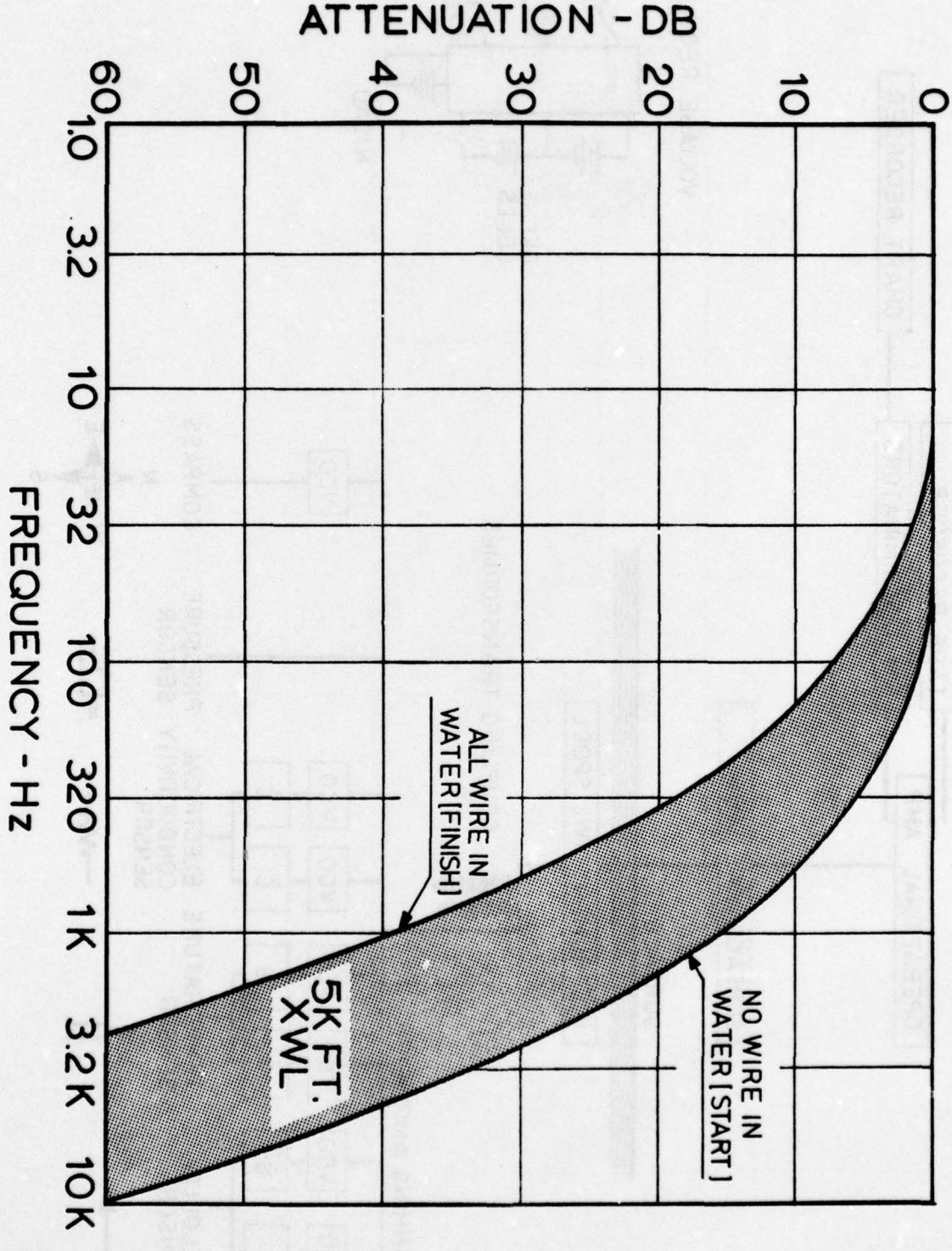
ATTENUATION - DB
0
10
20
30
40
50
60
FREQUENCY - Hz
1.0
3.2
10
32
100
320
1K
3.2K
10K
ALL WIRE IN WATER [FINISH]
NO WIRE IN WATER [START]
5K FT. XWL

Figure 6

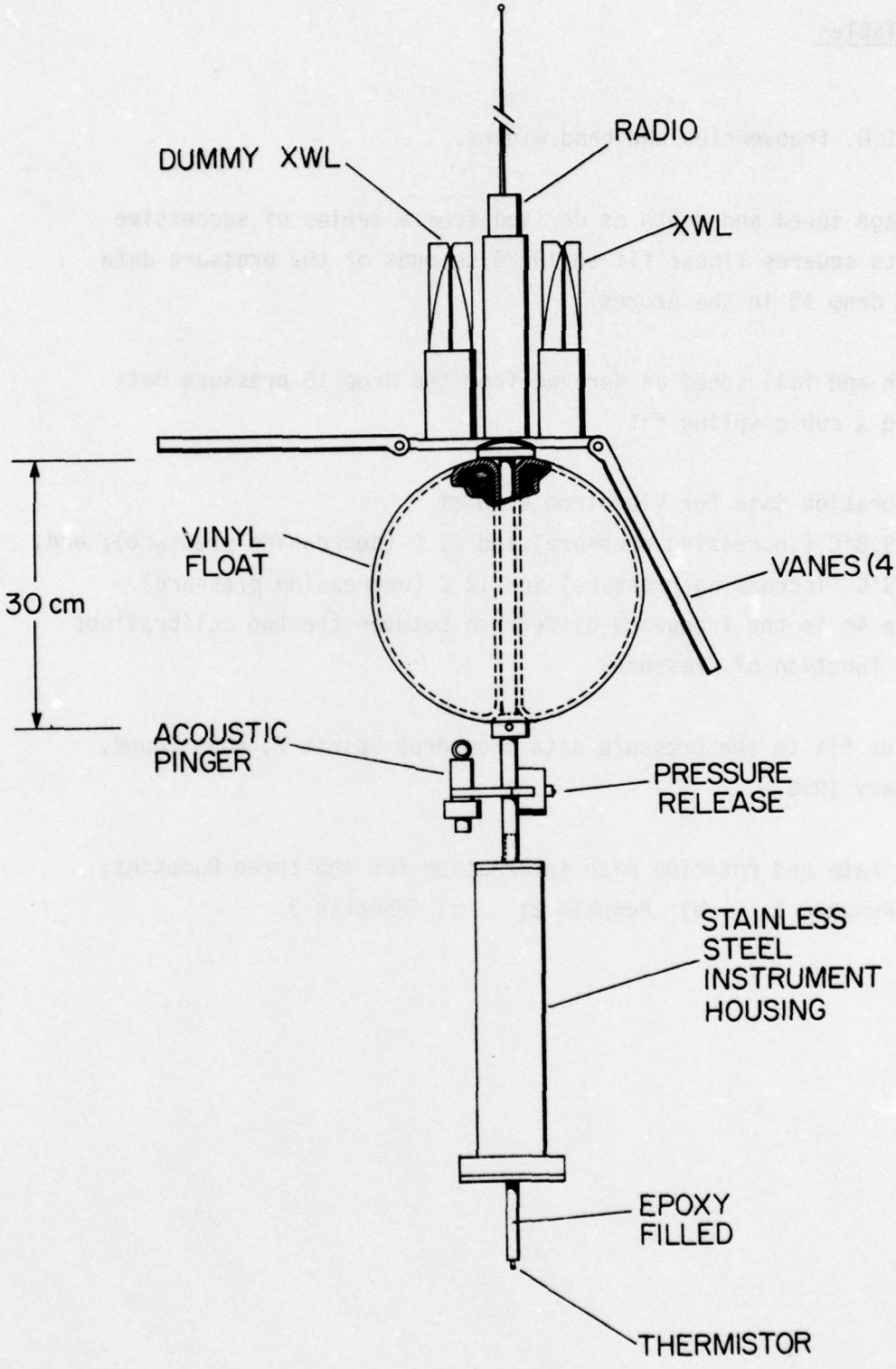
DUMMY XWL
RADIO
XWL
VINYL FLOAT
VANES (4)
30 cm
ACOUSTIC PINGER
PRESSURE RELEASE
STAINLESS STEEL INSTRUMENT HOUSING
EPOXY FILLED
THERMISTOR

Figure 7

List of Tables

1 I.R.I.G. frequencies and band widths.

2 Average speed and depth as derived from a series of successive leasts squares linear fit to 10.24 seconds of the pressure data from drop 15 in the Azores.

3 Depth and fall speed as derived from the drop 15 pressure data using a cubic spline fit.

4 Calibration data for Vibrotron 4193 at
a) 19.8°C (increasing pressure) and 21 C (decreasing pressure); and,
b) 13°C (increasing pressure) and 12 C (decreasing pressure).
Table 4c is the frequency difference between the two calibrations as a function of pressure.

5 Spline fit to the pressure data from drop Spirit 7, Howe Sound, January 1976.

6 Fall rate and rotation rate information for the three Pumpkins:
a) Pumpkin 1; b) Pumpkin 2; c) Pumpkin 3

Band	-7.5%	Centre Frequency	+7.5%	Modulation Frequency for ½db Attenuation.
1	370	400	430	6
2	518	560	602	8
3	675	730	785	11
4	888	960	1,032	14
5	1,202	1,300	1,398	20
6	1,572	1,700	1,828	25
7	2,127	2,300	2,473	35
8	2,775	3,000	3,225	45
9	3,607	3,900	4,193	59
10	4,995	5,400	5,805	81
11	6,799	7,350	7,901	110
12	9,712	10,500	11,288	160
13	13,412	14,500	15,588	220

Table 1

Depth m	Speed m/sec x 10	$\sum$ Speed	$\overline{\text{Speed}}$
-2.51253	4.14981	4.14981	4.14981
1.69070	5.04810	9.19791	4.59895
6.65703	4.65483	13.85273	4.61758
11.46871	5.45537	19.30780	4.82695
17.37750	5.09278	24.40057	4.88011
22.41380	5.35724	29.75760	4.95960
27.77602	4.99398	34.75177	4.95454
32.74113	5.64085	40.39261	5.04908
38.69653	5.17658	45.56918	5.06324
44.27657	5.21645	50.78563	5.07856
49.70020	5.13417	55.91980	5.08362
55.16338	5.16042	61.08021	5.09052
60.40262	5.56830	66.65451	5.12727
66.13673	5.04195	71.69644	5.12117
71.38210	5.33916	77.03560	5.13571
76.98781	5.16194	82.21755	5.13960
82.39137	5.36378	87.58130	5.15164
87.70808	5.15804	92.73993	5.15222
93.14868	5.27398	98.01390	5.15065
98.44304	5.04962	103.06351	5.15318
104.15855	5.02185	108.08536	5.17549
109.31653	5.55910	114.24491	5.19293
115.13246	5.16677	119.53127	5.18919
120.40249	5.39185	124.74312	5.19703
125.71230	5.29982	130.04292	5.20172
131.19696	5.28852	135.33144	5.20506
136.48499	5.44861	140.78004	5.21403
142.12866	5.21034	145.99038	5.21416
147.56758	5.39468	151.45505	5.22038
153.09463	5.10809	156.49313	5.21664
158.48630	4.97419	161.47731	5.20682
163.57308	4.78714	166.26445	5.19504
168.45888	5.44126	171.70171	5.20308
173.71645	5.24304	177.04474	5.20720
179.22556	4.90177	181.94650	5.19847
184.22443	5.30147	187.24797	5.20133
189.85359	5.05513	192.28310	5.19684
195.06523	5.24204	197.52513	5.19803
200.53957	5.02770	202.55283	5.19806
205.55987	5.41180	207.96461	5.19911
211.01230	5.40870	213.37331	5.20423
216.60590	5.30089	218.67419	5.20653
221.99858	5.13561	223.80980	5.20488
227.22061	5.37212	229.18192	5.20808
232.58070	5.45579	234.63770	5.21413
238.02425	4.22760	238.86348	5.19268
242.43082	5.43731	244.30078	5.19769
247.91618	5.11681	249.41757	5.19620
253.47461	4.99412	254.41168	5.19207
258.58203	5.30508	259.71729	5.19435
264.07471	5.24978	264.96704	5.19543
269.43872	5.36989	270.35609	5.19917
274.69355	5.08230	275.43856	5.19696
280.20068	5.36061	280.79956	5.19999
285.57373	5.32666	286.12622	5.20229
291.13965	5.16989	291.29590	5.20171
296.42749	5.23790	296.53369	5.20234
301.88086	5.21632	301.75000	5.20259
307.17773	5.51221	307.66221	5.20783
312.54370	4.97916	312.64121	5.20402
317.64209	5.38408	317.62524	5.20697
322.88159	5.63164	323.25684	5.21382
328.56421	5.20097	328.45776	5.21361
333.77686	5.40347	333.86108	5.21658
339.44800	5.13972	339.00073	5.21559
344.72192	5.39377	344.39429	5.21809
350.08545	5.24063	349.63477	5.21843
355.49023	5.32952	354.96411	5.22006
360.81396	5.60084	360.56982	5.22565
366.48462	5.01680	365.56643	5.22266
371.62134	5.44788	371.03418	5.22583
377.12354	5.30706	376.34106	5.22696
382.78491	5.08169	381.42261	5.22497
387.98291	5.34769	386.77026	5.22662
393.59229	5.18533	391.95557	5.22607
399.19604	5.11442	397.06982	5.22460
404.40899	4.99090	402.06055	5.22157
409.56836	5.27326	407.33374	5.22223
414.86108	5.18852	412.52222	5.22180
420.30957	4.77467	417.29688	5.21621
425.53301	5.32473	422.62158	5.21755
430.77222	5.12136	427.74292	5.21658
436.14673	5.23108	432.97388	5.21655
441.40503	5.09702	438.07080	5.21513
446.62012	5.20431	443.27466	5.21500
452.00024	5.31729	448.59180	5.21618
457.31689	4.99051	453.58228	5.21359
462.50737	5.27441	458.85669	5.21428
467.82368	5.29745	464.15405	5.21521
473.06689	4.87136	468.92539	5.21159
478.10620	5.11899	474.14429	5.21038
483.47632	5.12984	479.27393	5.20950
488.57959	5.43217	484.70605	5.21189
494.04663	4.98924	489.69531	5.20952
499.17822	5.16761	494.86279	5.20998
504.27759	5.47118	500.33374	5.21161
509.87378	4.94751	505.28125	5.20908
514.99679	5.24296	510.52417	5.20943
520.26489	5.19830	515.72241	5.20952
525.61084	5.03918	520.76147	5.20761
530.82007	5.01284	525.77417	5.20568
536.05371	5.17164	530.94580	5.20535
541.26050	5.50182	536.44751	5.20823
546.88652	5.36056	541.80766	5.20969
552.05420	5.49650	547.30420	5.21242
557.57056	5.30737	552.61157	5.21332
562.87163	4.96936	557.52075	5.21047
568.15430	5.15234	562.67285	5.20993
573.28711	5.42501	568.09766	5.21190
578.83472	5.15414	573.69171	5.21138
583.95532	5.34022	578.59180	5.21254
589.24658	5.33319	582.92480	5.21351
594.81445	5.17674	589.10132	5.21329
599.91748	4.87458	593.97583	5.21051
604.99341	5.24399	599.26978	5.21104
610.32715	5.31710	604.58667	5.21195
615.67993	4.92846	609.51489	5.20953
620.63818	5.61188	615.12671	5.21294
626.03247	5.24621	620.37280	5.21322
631.48267	4.97647	625.34912	5.21124
636.51807	5.19415	630.54321	5.21110
641.85913	5.13715	635.68018	5.21049
647.16626	5.21276	640.89282	5.21051
652.54590	5.02523	645.91797	5.20902
657.73022	5.13890	651.05664	5.20845
663.13940	5.10315	656.15967	5.20762
668.44409	4.95625	661.11572	5.20564
673.56323	5.00374	666.11938	5.20406
679.01489	5.07418	671.19336	5.20305
684.33276	4.90477	676.09750	5.20075
689.51587	5.22957	681.32739	5.20197
694.84375	5.23242	686.55981	5.20121
700.26343	4.92881	691.48853	5.19916
705.40088	5.02668	696.51514	5.19787
710.66382	5.34910	701.86401	5.19899
716.04639	5.22365	707.08765	5.19917
721.19067	5.52196	712.60938	5.20153
726.60474	5.34070	717.94995	5.20254
732.08838	4.96810	722.91797	5.20085
737.07768	5.24496	726.16284	5.20116
742.49683	4.76844	722.93115	5.19609

Table II

BEST AVAILABLE COPY

Depth m	Speed m/sec	Accel. m/sec^2
-3.82754	0.52532	0.0
1.54929	0.52510	0.00001
6.92685	0.52522	0.00002
12.30620	0.52547	0.00003
17.68878	0.52585	0.00004
23.07600	0.52632	0.00005
28.46819	0.52685	0.00005
33.86607	0.52743	0.00006
39.26985	0.52803	0.00005
44.67935	0.52854	0.00005
50.09415	0.52903	0.00004
55.51356	0.52945	0.00004
60.93698	0.52980	0.00003
66.36351	0.53006	0.00002
71.79230	0.53024	0.00001
77.22247	0.53033	0.00000
82.65336	0.53032	-0.00000
88.08316	0.53023	-0.00001
93.51190	0.53005	-0.00002
98.93835	0.52979	-0.00003
104.36162	0.52943	-0.00004
109.78073	0.52898	-0.00005
115.19479	0.52843	-0.00006
120.60278	0.52781	-0.00007
126.00398	0.52713	-0.00007
131.39764	0.52635	-0.00008
136.78339	0.52555	-0.00008
142.16069	0.52471	-0.00008
147.52930	0.52385	-0.00008
152.88918	0.52299	-0.00008
158.24019	0.52216	-0.00008
163.58305	0.52139	-0.00007
168.91353	0.52071	-0.00006
174.24762	0.52015	-0.00005
179.57146	0.51968	-0.00004
184.89132	0.51931	-0.00002
190.20726	0.51903	-0.00002
195.52086	0.51883	-0.00002
200.83240	0.51862	-0.00002
206.14236	0.51849	-0.00001
211.45131	0.51843	-0.00001
216.75934	0.51834	-0.00000
222.06699	0.51832	0.00000
227.37471	0.51836	0.00001
232.68318	0.51847	0.00001
237.99326	0.51867	0.00003
243.30602	0.51900	0.00004
248.62268	0.51943	0.00005
253.94421	0.51994	0.00005
259.27100	0.52049	0.00006
264.60400	0.52107	0.00006
269.94263	0.52164	0.00006
275.28711	0.52220	0.00005
280.63721	0.52273	0.00005
285.99243	0.52323	0.00005
291.35278	0.52369	0.00004
296.71753	0.52412	0.00004
302.08667	0.52450	0.00004
307.45947	0.52483	0.00003
312.83569	0.52511	0.00003
318.21556	0.52534	0.00003
323.59888	0.52552	0.00003
328.98511	0.52566	0.00003
334.37427	0.52576	0.00002
339.76587	0.52581	0.00002
345.15918	0.52582	0.00001
350.55347	0.52581	0.00000
355.94800	0.52580	-0.00000
361.34204	0.52578	-0.00001
366.73462	0.52575	-0.00002
372.12476	0.52569	-0.00003
377.51172	0.52557	-0.00004
382.89429	0.52539	-0.00005
388.27148	0.52481	-0.00006
393.64209	0.52414	-0.00007
399.00562	0.52339	-0.00008
404.36084	0.52258	-0.00008
409.70801	0.52175	-0.00008
415.04639	0.52091	-0.00008
420.37622	0.52010	-0.00008
425.69800	0.51932	-0.00007
431.01196	0.51857	-0.00007
436.31836	0.51786	-0.00007
441.61792	0.51719	-0.00006
446.91064	0.51659	-0.00006
452.19775	0.51604	-0.00005
457.47949	0.51557	-0.00004
462.75705	0.51519	-0.00003
468.03101	0.51490	-0.00002
473.30249	0.51469	-0.00002
478.57227	0.51457	-0.00001
483.84106	0.51453	-0.00000
489.11011	0.51455	0.00001
494.37939	0.51463	0.00001
499.64990	0.51477	0.00002
504.92212	0.51496	0.00002
510.19629	0.51518	0.00002
515.47314	0.51544	0.00003
520.75269	0.51571	0.00003
526.03491	0.51599	0.00003
531.32007	0.51627	0.00003
536.60791	0.51652	0.00002
541.89819	0.51674	0.00002
547.19067	0.51691	0.00001
552.48438	0.51701	0.00001
557.77881	0.51703	-0.00000
563.07300	0.51699	-0.00001
568.36646	0.51690	-0.00001
573.65894	0.51677	-0.00002
578.94971	0.51659	-0.00002
584.23853	0.51638	-0.00002
589.52515	0.51615	-0.00002
594.80933	0.51592	-0.00002
600.09131	0.51570	-0.00002
605.37109	0.51552	-0.00002
610.64917	0.51537	-0.00001
615.92603	0.51526	-0.00001
621.20215	0.51520	-0.00000
626.47754	0.51518	0.00000
631.75317	0.51521	0.00000
637.02930	0.51527	0.00001
642.30615	0.51538	0.00001
647.58423	0.51553	0.00001
652.86353	0.51569	0.00001
658.14453	0.51579	0.00002
663.42725	0.51595	0.00002
668.71118	0.51610	0.00001
673.99683	0.51625	0.00001
679.28394	0.51640	0.00001
684.57251	0.51652	0.00001
689.86230	0.51662	0.00001
695.15283	0.51670	0.00001
700.44434	0.51676	0.00000
705.73636	0.51680	0.00000
711.02808	0.51682	0.00000
716.32031	0.51681	-0.00000
721.61255	0.51679	-0.00000
726.90430	0.51676	-0.00000
732.19556	0.51672	-0.00000
737.48657	0.51669	-0.00000
742.77734	0.51667	-0.00000

Table III

BEST AVAILABLE COPY

Vibrotron Calibration #4193

Ambient Temperature	19.8°C		Temperature 21.0° C	
	f	Δf		Δf
0 PSI	15.3282 KHz		15.3269	
50	15.2411	87.1	15.2395	87.4
100	15.1533	88.8	15.1516	87.9
150	15.0653	88.0	15.0643	87.3
200	14.9761	89.2	14.9754	88.9
250	14.8868	89.3	14.8860	89.4
300	14.7970	89.8	14.7959	90.1
350	14.7074	89.6	14.7053	90.6
400	14.6159	91.5	14.6141	91.2
450	14.5233	92.6	14.5223	91.8
500	14.4309	92.4	14.4297	92.6
550	14.3377	93.2	14.3361	93.6
600	14.2436	94.1	14.2421	94.0
650	14.1482	95.4	14.1468	95.3
700	14.0543	93.9	14.0529	93.9
750	13.9585	95.8	13.9573	95.6
800	13.8618	96.7	13.8610	96.3
850	13.7644	97.4	13.7637	97.3
900	13.6665	97.9	13.6660	97.7
950	13.5678	98.7	13.5672	98.8
1,000	13.4680	99.8	13.4679	99.3

Table IVa

Vibrotron Serial #4193

Ambient Temperature	13°C		Temperature 12° C	
	f	Δf		Δf
0 PSI	15.3228 KHz		15.3228	
50	15.2373	85.5	15.2357	87.1
100	15.1498	87.5	15.1484	87.3
150	15.0615	88.3	15.0602	88.2
200	14.9732	87.3	14.9716	88.6
250	14.8843	88.9	14.8824	89.2
300	14.7944	89.9	14.7927	89.7
350	14.7038	90.6	14.7023	90.4
400	14.6129	90.9	14.6113	91.0
450	14.5213	91.6	14.5197	91.6
500	14.4288	92.5	14.4277	92.0
550	14.3361	92.7	14.3340	93.7
600	14.2417	94.4	14.2394	94.6
650	14.1485	93.2	14.1465	92.9
700	14.0558	94.7	14.0517	94.8
750	13.9577	97.1	13.9563	95.4
800	13.8616	96.1	13.8602	96.1
850	13.7648	96.8	13.7632	97.0
900	13.6664	98.4	13.6661	97.1
950	13.5679	98.5	13.5677	98.4
1,000	13.4687	99.2	13.4688	98.9

Table IVb

Pressure Psi	Δf Hz		
0	5.4	580	1.6
50	3.8	600	1.4
100	3.5	680	.3
150	3.8	700	.5
200	2.9	750	.8
250	2.5	800	.2
300	2.6	880	.4
350	3.6	900	.1
400	3.0	950	.1
450	2.0	1000	.7
500	2.1		

Table IVc

Depth m	Speed m/sec	Acceleration m/sec^2
10.07252	0.53566	C.0
12.83567	C.53567	C.CCCCC
15.59885	0.53572	C.CCCC2
18.36250	0.53584	C.CCCC3
21.12692	C.54CC3	C.CCCC5
23.89256	0.54031	C.CCCC6
26.65985	C.54CE8	C.CCCC8
29.42934	0.54116	C.CCC10
32.20148	C.54173	C.CCC12
34.97678	0.54239	C.CCC14
37.75568	0.54313	C.CCC15
40.53856	C.54394	0.CCC16
43.32570	C.544EC	C.CCC17
46.11736	0.54569	C.CCC18
48.91364	C.54EEC	C.CCC18
51.71458	0.54752	C.CCC18
54.52022	C.54842	C.CCC17
57.33041	C.5493C	C.CCC17
60.14502	C.55C15	C.CCC16
62.96364	0.55094	C.CCC15
65.78661	C.55169	C.CCC14
68.61307	0.55238	C.CCC13
71.44293	C.55303	C.CCC12
74.27597	0.55362	C.CCC11
77.11191	0.55417	C.CCC10
79.95055	C.55467	C.CCCC9
82.79163	C.55512	C.CCCC8
85.63490	C.55553	C.CCCC7
88.48012	C.55588	C.CCCC6
91.32706	0.55619	C.CCCC6
94.17545	C.55645	C.CCCC5
97.02505	0.55667	C.CCCC4
99.87564	0.55683	C.CCCC3
102.72694	C.55695	C.CCCC2
105.57875	0.55703	C.CCCC1
108.43085	C.55707	C.CCCC1
111.28310	0.55708	C.CCCC0
114.13535	0.55707	-C.CCCC1
116.98747	C.55703	-C.CCCC1
119.83932	C.55697	-C.CCCC1
122.69080	0.55688	-C.CCCC2
125.54176	C.55678	-C.CCCC2
128.39215	0.55665	-C.CCCC3
131.24182	C.55650	-C.CCCC3
134.09071	0.55634	-C.CCCC3
136.93872	C.55616	-C.CCCC4
139.78577	0.55597	-C.CCCC4
142.63175	C.55576	-C.CCCC4
145.47676	0.55555	-C.CCCC4
148.32063	C.55534	-C.CCCC4
151.16338	0.55513	-C.CCCC4
154.00500	C.55491	-C.CCCC4
156.84566	0.55469	-C.CCCC4
159.68506	0.55448	-C.CCCC4
162.52348	0.55426	-C.CCCC4
165.36079	0.55404	-C.CCCC4
168.19690	C.55384	-C.CCCC4
171.03210	C.55364	-C.CCCC4
173.86624	0.55347	-C.CCCC3
176.69965	0.55331	-C.CCCC3
179.53221	0.55319	-C.CCCC2
182.36441	0.55312	-C.CCCC1
185.19620	0.55309	C.CCCC0
188.02814	0.55311	C.CCCC1
190.86014	0.55317	C.CCCC1
193.69263	0.55325	C.CCCC2
196.52545	0.55335	C.CCCC2
199.35852	0.55345	C.CCCC2
202.19278	0.55355	C.CCCC2
205.02727	0.55364	C.CCCC2
207.86206	0.55372	C.CCCC1
210.69734	0.55378	C.CCCC1
213.53276	C.55383	C.CCCC1
216.36855	0.55387	C.CCCC1
219.20435	0.55390	C.CCCC1
222.04044	C.55392	C.CCCCC
224.87648	0.55394	C.CCCCC
227.71274	0.55395	C.CCCCC
230.54890	0.55396	C.CCCCC
233.38524	0.55396	C.CCCCC

Table V

BEST AVAILABLE COPY

Table VIa

Depth metres	Speed metres/s	Accel. metres/s^2
-8.96102	0.19001	0.0
-6.04349	0.18973	-0.00006
-3.14141	0.18776	-0.00020
-0.28576	0.18388	-0.00028
2.50539	0.17959	-0.00027
5.23427	0.17587	-0.00021
7.91288	0.17308	-0.00015
10.55629	0.17128	-0.00009
13.17939	0.17043	-0.00003
15.79596	0.17038	0.00002
18.41602	0.17084	0.00004
21.04556	0.17159	0.00005
23.68790	0.17249	0.00006
26.34540	0.17357	0.00008
29.02054	0.17476	0.00008
31.71385	0.17594	0.00008
34.42545	0.17714	0.00008
37.15634	0.17847	0.00009
39.90904	0.17997	0.00010
42.68614	0.18167	0.00012
45.49121	0.18362	0.00014
48.32819	0.18583	0.00015
51.20099	0.18826	0.00016
54.11169	0.19073	0.00016
57.05952	0.19307	0.00015
60.04175	0.19519	0.00013
63.05440	0.19701	0.00010
66.01938	0.19833	0.00007
69.14421	0.19911	0.00004
72.20609	0.19953	0.00002
75.27298	0.19978	0.00001
78.34251	0.19989	0.00000
81.41316	0.19992	0.00000

Rotation period 5.1 seconds

Table VIb

Depth metres	Speed metres/s	Accel. metres/s^2
-0.70479	0.17926	0.0
2.96830	0.17959	0.00004
6.65870	0.18098	0.00009
10.38495	0.18189	0.00008
14.14557	0.18422	0.00004
17.92438	0.18468	0.00001
21.70630	0.18460	-0.00001
25.48738	0.18476	0.00003
29.28139	0.18592	0.00008
33.10783	0.18784	0.00010
36.97670	0.18996	0.00010
40.88565	0.19167	0.00007
44.82274	0.19270	0.00003
48.77504	0.19324	0.00002
52.73759	0.19373	0.00002
56.70929	0.19408	0.00001
60.68358	0.19392	-0.00003
64.64723	0.19304	-0.00006
68.58575	0.19146	0.00010
72.48441	0.18915	-0.00013
76.32916	0.18624	-0.00015
80.11241	0.18330	-0.00013
83.84303	0.18124	-0.00007
87.54626	0.18066	0.00001
91.25273	0.18149	0.00007
94.98636	0.18321	0.00010
98.75867	0.18517	0.00009
102.56902	0.18686	0.00007
106.40878	0.18801	0.00004
110.26616	0.18860	0.00002
114.13089	0.18877	0.00000
117.99681	0.18875	-0.00000
121.86194	0.18870	-0.00000
125.72600	0.18866	-0.00000
129.58965	0.18865	0.00000

Rotation period 4.8 seconds

Table VIc

Depth metres	Speed metres/s	Accel. metres/s^2
-7.62374	0.18296	0.0
-3.87653	0.18300	0.00001
-0.12697	0.18321	0.00002
3.62917	0.18364	0.00003
7.39661	0.18431	0.00004
11.17986	0.18518	0.00005
14.98293	0.18624	0.00005
18.80884	0.18740	0.00006
22.65907	0.18859	0.00006
26.53339	0.18974	0.00005
30.43034	0.19080	0.00005
34.34764	0.19173	0.00004
38.28264	0.19253	0.00004
42.23262	0.19319	0.00003
46.19501	0.19374	0.00002
50.16737	0.19417	0.00002
54.14769	0.19451	0.00001
58.13403	0.19476	0.00001
62.12465	0.19493	0.00001
66.11780	0.19501	0.00000
70.11183	0.19502	-0.00000
74.10535	0.19496	-0.00000
78.09721	0.19486	-0.00001
82.08627	0.19469	-0.00001
86.07140	0.19448	-0.00001
90.05194	0.19424	-0.00001
94.02759	0.19400	-0.00001
97.99832	0.19377	-0.00001
101.97451	0.19356	-0.00001
105.92686	0.19339	-0.00001
109.88626	0.19327	-0.00000
113.84369	0.19320	-0.00000
117.80008	0.19317	-0.00000

Rotation period 4.6 seconds